Fall 2011

Multiple differential study of fragmentation processes in 75 keV proton-molecular hydrogen collisions

Kisra Nayomal Egodapitiya

Follow this and additional works at: https://scholarsmine.mst.edu/doctoral_dissertations

Part of the Physics Commons

Department: Physics

Recommended Citation

MULTIPLE DIFFERENTIAL STUDY OF FRAGMENTATION PROCESSES IN 75

keV PROTON - MOLECULAR HYDROGEN COLLISIONS

by

KISRA NAYOMAL EGODAPITIYA

A DISSERTATION

Presented to the Faculty of the Graduate School of the

MISSOURI UNIVERSITY OF SCIENCE AND TECHNOLOGY

In Partial Fulfillment of the Requirements for the Degree

DOCTOR OF PHILOSOPHY
in
PHYSICS

2011

Approved
Michael Schulz, Advisor
G.D. Wadill
D.H. Madison
J.L. Peacher
V. Samaranayake

PUBLICATION DISSERTATION OPTION

This dissertation has been prepared in the style utilized by journals Physical Review Letters and Physical Review A. Pages 14-26 were published in Physical Review Letters and pages 27-50 were published in Physical Review A. Sections 1, 2, and 3 have been added for purposes normal to dissertation writing.

ABSTRACT

Double Differential Cross Sections (DDCS) were measured for single ionization of H_2 by 75 keV proton (p) impact as a function of the projectile scattering angle (θ_p) for a fixed energy loss (ΔE) for two different target-collimating slit distances, which determined the width of the projectile wave packet (Δx). In one case Δx was larger than the inter-nuclear separation of the H_2 molecule (coherent projectile beam), while for the other case it was much smaller than the inter-nuclear separation (incoherent projectile beam). A Young type interference pattern was observed in the coherent data, but this was not present in the incoherent data. The results imply that the projectile coherence can have a clear effect on measured cross sections and that the experimental beam preparation must be incorporated in the theoretical treatment. Moreover Single Differential Cross Section (SDCS) were measured for single electron capture by 75 keV proton impact on H_2, and here, too, a similar effect was observed. Furthermore SDCS for single electron capture by 25 keV proton impact on H_2 and He targets also revealed interference structures, qualitatively different from the Young type interference structures seen at 75 keV proton energy. Structures for the Helium target imply that the effect of projectile coherence can be present for atomic targets as well.

In a previous experiment, it has been shown that these Young type interference structures are to a large extent independent of ΔE. This suggests that they should also be independent of the process occurring in the collision. To test this DDCS were measured for dissociative ionization for 75 keV proton impact on H_2 as a function of θ_p for four ΔE values. Additional structures compared to non dissociative ionization were observed.

ACKNOWLEDGMENTS

First of all, I would like to convey my heartfelt gratitude to my advisor, Dr. Michael Schulz. My accomplishments as a physicist would not have been possible without your immense guidance, encouragement, and support. Next, I would like to thank Dr. Ahmad Hasan who helped me in every possible way to excel in my work. It was a wonderful learning experience with you. I would also like to thank my friends and colleagues in the lab, Jason Alexander, Aaron Laforge, Sachin Sharma, Thusitha Arthanayake, and Giorgi Sakhelashvili. Further, my gratitude goes to our collaborators Dr. Don Madison and Dr. Robert Moshammer.

I sincerely thank my committee members Dr. Don Madison, Dr. Jerry Peacher, Dr. Dan Waddill, and Dr. V. Samaranayake. I highly appreciate the support you have given me in many ways. I must thank all the professors in the physics department, who taught me numerous courses. I was very fortunate to have extremely skillful teachers like you.

Further, I like to thank the staff members in the physics department, Pam Crabtree, Ellen Kindle, Charlie McWhorter, Russ Summers, and Brian Swift for their support. I am grateful to all the graduate students in the physics department for making my time in Rolla enjoyable.

Finally, I thank my loving wife, Irangi, and my family for all their patience, sacrifices, and support. I could not have done this without you.

TABLE OF CONTENTS

LIST OF ILLUSTRATIONS

1. INTRODUCTION

Collisions of atoms and molecules with charged particles play a crucial role in understanding nature. To understand natural phenomena one has to address two fundamental aspects. First, the forces acting between pairs of particles must be known, which is a focus of high energy physics. Secondly, how a system of more than two particles evolves under the influence of these forces must be known. For a system containing two particles, which are interacting with each other, one can find an exact solution provided that the underlying force is fully understood. This means for a microscopic system, one has to solve Schrödinger's equation (or the Dirac/Klein-Gordon equation for relativistic cases). However it turns out that if at least one more particle is added to this system, an exact analytic solution becomes impossible even if the forces are precisely known. This is one of the yet unsolved, fundamentally important problems in physics, and is known as the few body problem. Because of this difficulty one has to resort to heavy modeling, and to test the accuracy of these models, detailed experiments must be performed.

For a number of reasons atomic collisions provide the best test cases to study few body dynamics [1-3]. First, in atomic collisions the forces acting between the particles is the electromagnetic force, which is very well understood. Therefore any discrepancy between theory and experiment can be attributed to the description of the few body dynamics. In contrast, in e.g. nuclear reactions, the force involved is the strong force (and, to a lesser extent, the weak force), which is not nearly as well understood as the electromagnetic force. Therefore, it is not clear whether any discrepancies, which may occur, are due to an incomplete understanding of the few body dynamics or due to the

inaccurate representation of the underlying force. Second, in atomic reactions the number of particles involved can be kept small, and the momenta of all the particles in the final state can be measured. In contrast, if one studies a solid state system, for which the underlying force is also the electromagnetic force, it is impossible to measure the momenta of the final state on an individual particle level, and one can only measure statistically averaged or collective quantities instead. A potential lack of understanding can be hidden in the statistics, which could result in misleadingly good agreement between experiment and theory.

In experimental atomic collision studies cross sections are typically measured for a particular reaction and are compared with theoretical predictions. Cross sections differential with respect to one or more parameters, such as scattering angles, energy losses and momenta, are more sensitive to the few body dynamics than total cross sections. For example, FDCS (cross sections which are differential with respect to all observables in the final state) measured for ion impact, revealed that something fundamental is missing in the fully quantum mechanical theory. In the following we will discuss one such example, where FDCS were studied for 100 MeV/a.m.u. C^{6+} on He collisions. The comparison of these results with theoretical models, which incorporated nuclear-nuclear scattering either classically or quantum-mechanically, revealed that projectile coherence might be the cause for some of the significant discrepancies that have been observed between experiment and theory. The results of that experiment and their implications will be discussed in the following because the work presented in this thesis is directly related to these implications.

To extract FDCS one has to know the momentum of all the particles in the final state. For example, in a single ionization experiment the momenta of three particles must be known and this can be done by measuring the momentum of two particles directly and the third momentum can be deduced using the kinematic conservation laws. For electron impact experiments, FDCS have been available for several decades. This has been done by directly measuring the momenta of the scattered electron and of the ejected electron [4-5]. However these experiments, which were done using traditional electron momentum spectrometers, were limited to a small fraction of the 4π solid angle of the momentum space. Further, it was not possible to use this method for fast heavy ion impact experiments because there the achievable resolution in the projectile momentum was not sufficient. The development of COLd Target Recoil Ion Momentum Spectroscopy (COLTRIMS) [6] and subsequent reaction microscopes [7] opened up a new era in atomic collisions. With this technique the measurement of FDCS for ion impact became feasible [2, 8-12] even for large projectile energies. This is done by measuring the recoil ion momentum with a coincidence set up with either the ejected electrons or the scattered projectile [9].

This technique enabled the measurement of FDCS over the complete three dimensional space, first for ion impact [2] (for recent reviews see [3, 13]), and later for electron impact experiments [14]. These studies revealed severe discrepancies with theory [3, 13, 14]. Prior to these results collision systems with small perturbations η (ratio between projectile charge and velocity) were thought to be well understood, such that even the First Born Approximation (FBA) was thought to give an adequate description of the ionization process. But it turns out that even for these systems there are
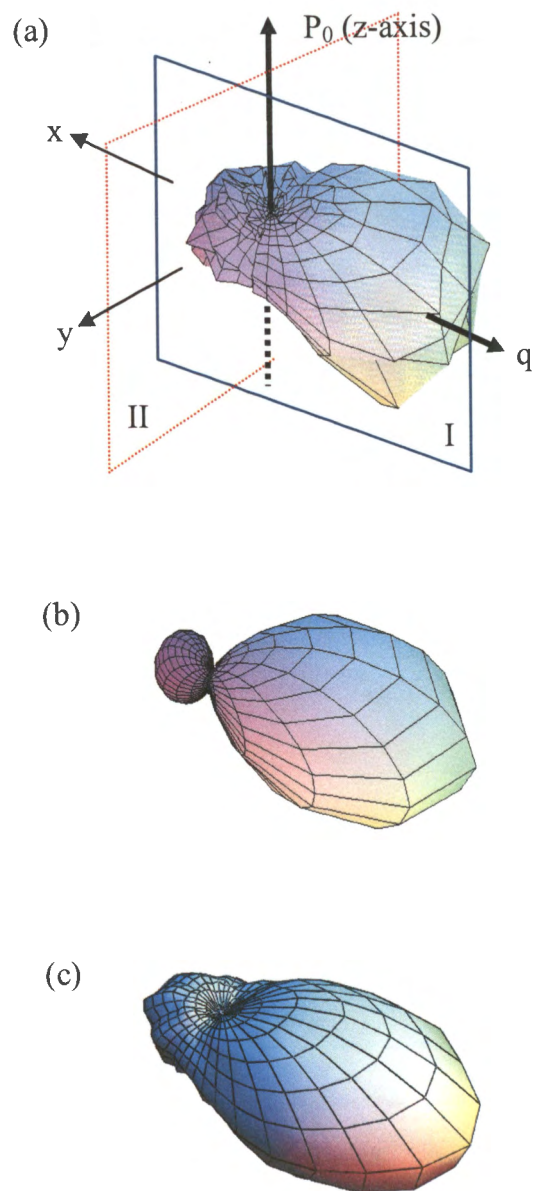
Figure 1.1 Experimental and theoretical three dimensional FDCS for ionization of He by 100 MeV/a.m.u. C^{6+}. (a) Experimental Cross sections (b) 3DW calculations (c) FBA convoluted with classical elastic scattering for N-N interaction.

severe discrepancies between theory and experiment. These discrepancies were more severe for ion impact than for electron impact. For electron impact, several sophisticated non-perturbative models have been developed over the last decade [e.g. 1, 15-17], and these have been able to reproduce experimental data at least qualitatively although some quantitative disagreements remain [14]. For ion impact such calculations are just starting to emerge [18-20]. However, for ion impact severe discrepancies remain even for the non-perturbative approaches [20].

In Figure 1.1-a FDCS are shown for single ionization of He by 100 MeV/a.m.u. C^{6+} impact in terms of a three dimensional angular distribution of the ejected electrons with all other kinematic parameters fixed.

Here $\mathbf{p_0}$ is the initial projectile momentum and $\mathbf{q}$ is the momentum transfer, which is defined as the difference between the initial and final projectile momentum. Figure 1.1-b shows a fully quantum mechanical state of the art three body distorted wave calculation (3DW) [21], which takes higher order interactions into account. More specifically, the 3DW model incorporates a quantum mechanical treatment of the nuclear-nuclear interaction. In the calculation a pronounced double lobe structure, well known from FDCS measurements for electron impact, can be seen. The larger contribution towards the momentum transfer $\mathbf{q}$ is called the binary peak and the contribution opposite to momentum transfer is called the recoil peak. The binary peak is due to a hard collision between the projectile and the electron. The electron is emitted in the direction of $\mathbf{q}$ while the recoil ion remains essentially passive. The recoil peak occurs because of the back scattering of the ejected electron from the target nucleus, transferring some momentum to the recoil ion. Surprisingly, the 3DW model cannot reproduce the

experimental data very well [2,22]. The theory predicts a sharp minimum between the two lobes, but in the experiment this is completely filled up. Even more surprisingly when the FBA was convoluted with classical elastic scattering due to the nuclear-nuclear interaction, there was excellent agreement between theory and experiment (figure1.1-c) [22]. This convolution is done in three steps. In the first step an event file containing momentum vectors for the particles in the final state is generated using a Monte Carlo method. The frequency of occurrences of specific momentum configurations reflect the FDCS calculated using the FBA. In the second step the momentum transfer from classical elastic scattering is added to the momentum transfer obtained from the FBA event by event from the file generated in the first step. Finally, FDCS are extracted in the same way as it is done with the experimental data, which are contained in an event file of essentially the same structure as the theoretical event file.

Interestingly, all fully quantum mechanical calculations have the same problem as the 3DW model. This suggests that all the fully quantum mechanical calculations might have a fundamental problem in common. One feature that all of these models share is that they represent the projectile as a delocalized wave, or in other words, the projectile is fully coherent. This means that the width of the projectile wave packet is larger than the target atom dimension. On the other hand, in the classical treatment described above the projectile is completely localized as far as the nuclear-nuclear interaction is concerned because it assumes well defined projectile trajectories. In the experiment the width of the projectile wave packet depends on the experimental conditions and for this particular experiment the width of the projectile wave packet was much smaller than the target size. This suggests that the reason for this discrepancy might be due to the fact that in the

theory the projectile coherence is not properly accounted for. In the theory the projectile is coherent while in the experiment, discussed here it is incoherent. But in scattering theory, to represent a projectile in terms of a localized wave packet is extremely difficult. This is the reason for approximating the projectile by a delocalized wave (e.g. plane wave in the Born series). For electron impact experiments it turns out that the width of the projectile wave packet is almost always larger than the target dimension and therefore treating the projectile as fully coherent represents a realistic approximation. But in ion impact experiments as mentioned above, it is often a very unrealistic assumption. Therefore it is very important to investigate the possible influence of the projectile coherence on cross sections. In the first part of this thesis we will discuss an atomic collision version of Young's double slit experiment designed to test this fundamentally important aspect of formal scattering theory.

Young type interference structures due to indistinguishable scattering from the two atomic centers of the molecule were first predicted about fifty years ago by Tuan and Gerjuoy [23]. The first experimental evidence confirming this prediction was produced about thirty years later [24]. Later, interference patterns were observed in double differential electron energy spectra for ionization of H_2 by highly charged ion impact [25-27], where it was argued that the interference was due to indistinguishable emission of electrons from either of the two atomic centers of the molecule. However these structures were weak, and only after normalizing to theoretical calculation for atomic hydrogen, these became discernable. Later more pronounced interference structures were found for capture cross sections as a function of the molecular orientation in $He^{2+} + H_2$ collisions [28] and in fully differential recoil-ion momentum spectra for capture in $H_2^+ + He$

collisions [29]. Since both of these processes did not involve the ejection of an electron,

in these experiments it is the coherent scattering from the atomic centers which causes the

interference. Finally DDCS were measured for fixed projectile energy losses as a

function of the projectile scattering angle [30] for single ionization of molecular

hydrogen by 75 keV proton impact. In this case both types of interferences can be

present, however kinematic conditions were chosen such that the interference structure

was not affected much by the ejected electron energy.

As mentioned above for such an interference pattern to be present the width of the

projectile wave packet must be larger than the target dimension. Figure 1.2 shows a

schematic diagram of the optical Young's double slit experiment.
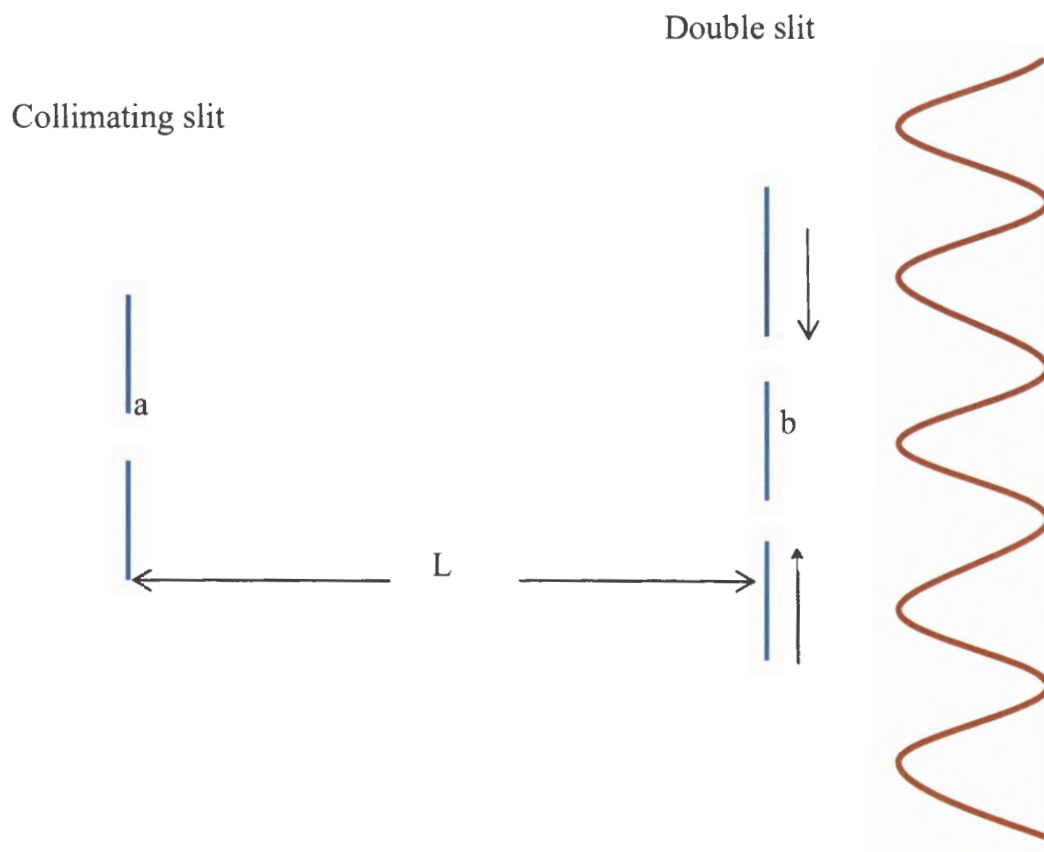
Figure 1.2 Schematic diagram of optical Young's double slit experiment.

Here a double slit separated by a distance b is illuminated by monochromatic light, and the resulting wave pattern is observed on a screen. To see an interference pattern the light falling on the double slit must be coherent. This means the width of a single photon wave packet Δx must be larger than the slit separation b. To accomplish this, a collimating slit of width a is placed at a distance L away from the double slit. The width Δx of the photon wave packet is then given by $\Delta x = 1/2 \, \lambda \, L/a$.

If L is small enough so that Δx is smaller than b, only one slit will be illuminated at a time and an interference pattern will not be present. However, if L is large so that Δx is larger than b, both slits will be illuminated simultaneously and an interference pattern can be visible. This idea can be used to test the role of the projectile coherence in an atomic collision version of Young's double slit experiment. To do this, the double slit is replaced by a Hydrogen molecule and the light beam is replaced by a proton beam. For small values of L, where Δx is smaller than the atomic separation, only one atom will be illuminated, i.e. the projectile can only get scattered from one atomic center of the molecule, and an interference pattern will not be present (figure 1.3-b). On the other hand for large L, so that Δx is larger than the atomic separation both atoms will be illuminated simultaneously and an interference pattern is expected (figure 1.3-a).

One important feature here is that the amplitude of the interference pattern for optical Young's double slit experiment, as shown in figure 1.2, remains nearly constant, compared to the central fringe. In contrast, in the atomic collision version of the Yong's double slit experiment the amplitude drops rapidly (figure 1.3) with the scattering angle. The reason for this is that, unlike in the optical case, in atomic scattering the incoherent amplitude drops rapidly with the scattering angle which causes the interference

oscillation to also drop rapidly (since the interference oscillation is the incoherent amplitude modulated by an interference term, which will be discussed in more detail in the following).
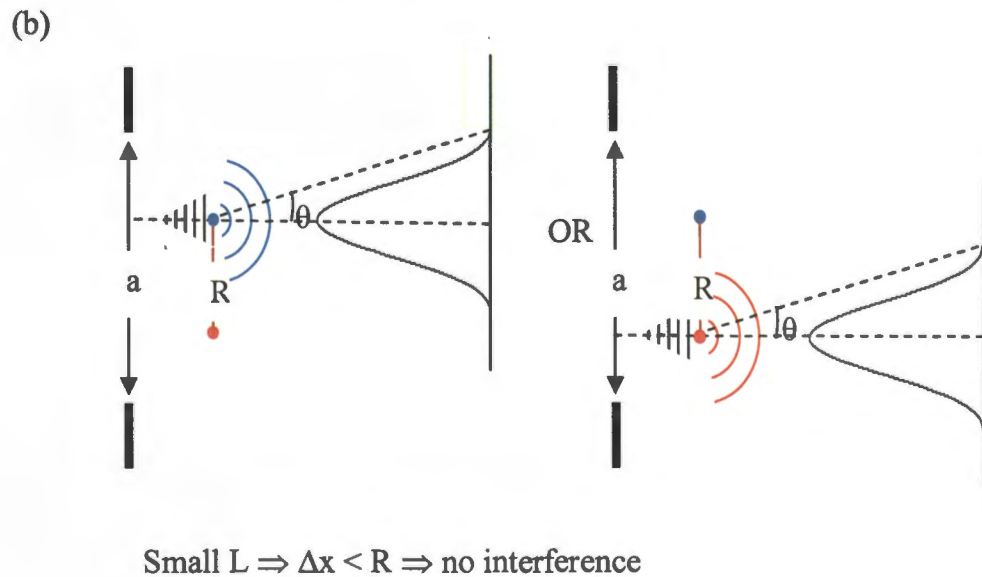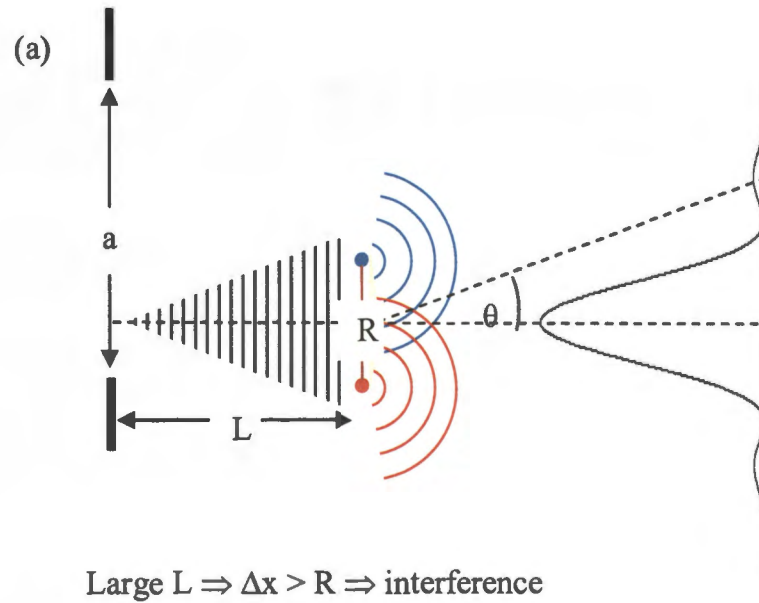
Figure 1.3 Atomic collision version of Young's double slit experiment.

Such an atomic version of Young's double slit experiment, in which the role of the projectile coherence was investigated, is presented in Paper I starting on page 14 of this dissertation.

As discussed earlier Young type interference structures were previously observed [30] in the DDCS for single ionization of H_2 by 75 keV proton impact, as a function of the projectile scattering angle, for fixed projectile energy losses (or equivalently the ejected electron energy). There, an interference structure was found as a function of the projectile scattering angle. On the other hand those structures were to a large extent independent of the ejected electron energy. The aim of the second project of this dissertation was to study to what extent Young's double slit type of interference structures depend on the specific scattering process.

In analogy to optical Young double slit interference, the DDCS for a coherent projectile beam can be written as the DDCS for an incoherent projectile beam multiplied by the interference term (IT) where,

$$IT = 1 + \cos \varphi \tag{1}$$

Here φ is called the phase angle and is given by $\varphi = \mathbf{p}_{rec} \cdot \mathbf{D}$, and $\mathbf{p}_{rec}$ is the recoil momentum and $\mathbf{D}$ is the position vector of one atomic center in the molecule with respect to the other. From momentum conservation it follows that the recoil momentum $\mathbf{p}_{rec}$ is given by $\mathbf{p}_{rec} = \mathbf{q} - \mathbf{k}_e$, where $\mathbf{k}_e$ is the momentum of the ejected electron. For the relatively small ejected electron energies considered in this experiment, $k_e \ll q$ except for small

scattering angles. For example, for scattering angles larger than 1 mrad, the corresponding q is larger than 3-3.5 a.u. whereas k_e is about 1 a.u. Therefore here, $k_e \ll q$ is a good approximation. This implies that the phase angle of the interference term will depend mostly on the momentum transfer **q**. The momentum transfer **q** is the vector sum of the longitudinal component ($\mathbf{q}_\parallel$) and the transverse component ($\mathbf{q}\perp$),

$$\mathbf{q} = \mathbf{q}_\parallel + \mathbf{q}\perp \tag{2}$$

Using the kinematic conservation laws it can be shown [6] that to a very good approximation the longitudinal component,

$$q_\parallel = (-Q+E_e)/v_p \tag{3}$$

Here Q is the Q-value of the reaction which is equal to the change in binding energy, E_e is the ejected electron energy and v_p is the projectile speed. The transverse component,

$$q\perp = p_0 \sin \theta \tag{4}$$

Here p_0 is the magnitude of the initial projectile momentum and θ is the projectile scattering angle. Q appears explicitly, only in $q_\parallel$ (equation 3). For different processes Q is different, but Q/v_p is typically small and therefore the contribution of q to the total q will be small. So, $q_\parallel$ will be small compared to $q\perp$ provided that E_e (or equivalently k_e) is small, which is a true assumption in this experiment. Hence, for a given scattering angle

(which is equivalent to the transverse momentum transfer, $q_\perp$ (see equation 4)) the interference term will not be affected much by Q. Therefore, one can expect that the interference pattern, with respect to the scattering angle will be essentially the same for different processes. The second paper of this dissertation, starting on page 28 will describe an experiment performed to investigate whether an interference pattern can be observed in the DDCS for ionization accompanied by fragmentation (dissociative ionization DI) by 75 keV proton impact and, if it does occur, whether it is similar to the structures observed in non-dissociative ionization of H_2 by the impact of 75 keV protons.

1. Manipulating Atomic Fragmentation Processes by Controlling the Projectile Coherence

K. N. Egodapitiya[1], S. Sharma[1], A. Hasan[2], A. C. Laforge[1], D. H. Madison[1], R. Moshammer[3], and M. Schulz[1]

[1]Department of Physics and LAMOR, Missouri University of Science & Technology, Rolla, Missouri 65409, USA
[2]Department of Physics, UAE University, P.O. Box 17551, Alain, Abu Dhabi, United Arab Emirates
[3]Max-Planck-Institut für Kernphysik, Saupfercheckweg 1, 69117 Heidelberg, Germany

We have measured the scattering angle dependence of cross sections for ionization in $p + H_2$ collisions for a fixed projectile energy loss. Depending on the projectile coherence, interference due to indistinguishable diffraction of the projectile from the two atomic centers was either present or absent in the data. This shows that, due to the fundamentals of quantum mechanics, the preparation of the beam must be included in theoretical calculations. The results have far-reaching implications on formal atomic scattering theory because this critical aspect has been overlooked for several decades.

When Rutherford introduced the concept of a scattering cross section [1], he had in mind a quantity which only depended on the properties of the colliding particles and the collision energy, but not on the experimental conditions such as the target density or the preparation of the projectile beam. However, since the advent of quantum mechanics, we know that an experiment providing information about the system of interest generally alters the system through the observation process. In a strict sense it is thus not possible to define an observable quantity which only depends on the properties of the system, but not on the observation process. Here, we are particularly interested in the consequences of these properties of quantum mechanics for scattering theory, which, in turn, directly deals with the fundamentally important and yet unsolved few-body problem (FBP) [2,3].

One implication of the above analysis for scattering theory is that the projectile should be represented in terms of a three-dimensionally localized wave packet with finite width which depends on the preparation of the beam. This is, however, a challenging task. Therefore, as an approximation the projectile is usually described as a delocalized particle [4], for example, in terms of a plane wave in the Born expansion [5]. In the vast majority of collision experiments analyzed so far this seemed to be a very well justified approximation. For electron impact collisions, for example, the width of the projectile wave packet is almost always large compared to the target dimension. But for ion impact the width of the wave packet can become similar or small compared to the target dimension for large collision energies. However, the projectile parameters which would be sensitive to the beam preparation (scattering angle and energy loss) are very difficult to measure directly and those experiments which determined the scattering angle under these conditions measured single differential cross sections (e.g., [6]). Such data are

probably not sufficiently sensitive to reveal any influence of the finite width of the projectile wave packet on the cross sections. Indeed, for decades of atomic collision research, the assumption of a delocalized projectile did not seem to pose a significant problem.

With the development of cold target recoil-ion momentum spectroscopy (COLTRIMS) [7,8], the sensitivity at which theoretical models can be tested has been significantly enhanced. More specifically, COLTRIMS made possible the measurements of fully differential cross sections (FDCS) for target ionization for the complete three-dimensional space (e.g., [2, 9-11]). These studies revealed unexpected discrepancies between experiment and theory, which were particularly surprising for small perturbations η (projectile charge to speed ratio). There, even the first Born approximation (FBA) was believed to provide a good description of the ionization process. The FBA strictly demands that the fully differential angular distribution of ejected electrons must be cylindrically symmetric about the momentum transfer vector $\mathbf{q}$ (difference between the initial and final projectile momenta) (e.g., [10]). In the experiments, in contrast, clear signatures of a breaking of this symmetry were observed. These qualitative discrepancies persisted even in nonperturbative approaches [12]. Even more surprising, an FBA calculation convoluted with classical elastic scattering between the projectile and the residual target ion, where the projectile was completely localized as far as the projectile–residual target ion interaction is concerned, reproduces the data very well [13]. These observations suggest that the difficulties of the fully quantum-mechanical calculations for ion impact originate, at least partly, from the assumption of a

delocalized projectile. This shortcoming of formal scattering theory has been completely overlooked for decades.

In this Letter we report experimental evidence that the localization of the projectile can have a significant and qualitative impact on atomic collision cross sections involving ionic projectiles. An atomic collision version of Young's double slit experiment was performed. Diffraction of a proton beam from the atomic centers of H_2 was studied in ionizing collisions. Depending on the coherence of the incoming projectile beam an interference pattern was either present or absent in the scattering angle dependence of the ionization cross sections. These results show that major parts of formal ion-atom scattering theory have to be revised.

To observe an interference pattern requires that the incoming projectile wave is coherent in two respects: first, since the phase difference between the waves diffracted from the atomic centers depends on the proton energy, the inherent energy spread ε must be sufficiently small. This can be expressed in terms of the longitudinal coherence length $\Delta z \approx (2\Delta p_z)^{-1} = v/2\varepsilon$ [14] (in atomic units a.u.), which must be on the order of or larger than the inter-nuclear separation D. Here, v is the projectile speed. Second, the width of the proton wave packet, its transverse coherence length Δr, must be large enough to illuminate both atomic centers simultaneously; i.e., Δr must also be larger than D. Δr can be manipulated by a collimating slit of width a at a distance L before the target region and is of the order of $\lambda L/(ka)$ (e.g., [15,16]). Here, λ is the de Broglie wavelength and k is a dimensionless constant which depends on the shape of the projectile wave packet. For a Gaussian wave packet $k = 2\pi$, but k=1 [15] and $k=2^{1/2}/\pi$ [16] have also been used in Δr. Here, we assume k = 3, as an approximate average of these values, to estimate Δr. If L is

small enough so that $\Delta r < D$ only one proton in the molecule is illuminated at a time. The projectile is then scattered incoherently and no interference structure is expected. If, on the other hand, L is large enough so that $\Delta r > D$ the projectile is coherently scattered, which can result in an observable interference pattern. Such structures have been predicted several decades ago [17] and reported recently [18,19]. [Interferences in the electron energy spectra due to coherent ejection from the two atomic centers were also reported (e.g., [20, 21]).]

In the experiment, a 75 keV proton beam, with an energy spread much smaller than 1 eV, was crossed with a neutral molecular hydrogen beam. The projectile beam was collimated by a set of slits 0.15 by 0.15 mm in size located at a variable distance L before the target region. The recoiling H_2^+ ions were extracted by an electric field of about 50 V/cm and detected by a channel-plate detector. The scattered protons passed through a switching magnet, to separate them from neutralized projectiles, and decelerated to 5 keV. The projectiles were then energy analyzed by an electrostatic parallel-plate analyzer and detected by a two dimensional position-sensitive channel-plate detector. The entrance and exit slits were long (approximately 2.5 cm) in one direction (the x direction), but narrow (75 μm) in the y direction, which is in the plane of dispersion. Therefore, all ionization events leading to scattering angles between 0 and 1.5 mrad were recorded simultaneously. Data were taken for a fixed projectile energy loss ΔE of 30 eV where a pronounced interference structure was observed earlier [19]. The projectile detector was set in coincidence with the recoil-ion detector.

Data were taken for two different slit-target distances L under otherwise identical experimental conditions. The larger distance, L = 50 cm, corresponds to a transverse

coherence length of $\Delta r \approx 2.2$ a.u., which is larger than the internuclear separation in the molecule ($D=1.4$ a.u.). Therefore, for this L the projectile beam is coherent. An incoherent projectile beam is realized with the smaller distance of $L = 6.5$ cm, corresponding to $\Delta r \approx 0.3$ a.u. The angular resolution for the projectiles was measured for both L with the target gas taken out and the energy analyzer set for $\Delta E = 0$. The same angular width (0.1 mrad full width at half maximum FWHM) was found for both L. Furthermore, the effect of the resolution in angle and energy-loss (3 eV FWHM) on the measured cross sections was tested using a Monte Carlo simulation [22]. Only at angles smaller than 0.1 mrad an observable, but small effect was found.

At smaller pass energies of the projectile energy analyzer than used in this experiment a resolution of less than 1 eV FWHM is achieved. Using this as an upper limit for the energy spread of the proton beam, the longitudinal coherence length is more than an order of magnitude larger than D; i.e., longitudinal coherence is always realized, regardless of L. However, to see interference in the θ dependence of the ionization cross sections requires both transverse and longitudinal coherence, so that no interference structure is expected at the small L.

Since the x position on the projectile detector defines the scattering angle θ and data were taken for a fixed ΔE, the coincident projectile position spectrum is directly proportional to the double differential cross section DDCS = $d^2\sigma/d(\Delta E)d\Omega_p$ for target ionization. The data were normalized to the single differential cross section $d\sigma/d(\Delta E)$ calculated using the semiempirical model by Rudd et al. [23]. These normalized DDCS are shown in Fig. 1 as a function of scattering angle for $L_1 = 50$ cm (closed symbols) and $L_2 = 6.5$ cm (open symbols). Significant differences between the data sets for the two

distances are quite obvious. At small θ the DDCS for large L (in the following referred to as the coherent data $DDCS_{coh}$) are about a factor of 2 larger than those for small L (incoherent data $DDCS_{inc}$), at intermediate θ ($\approx$ 0.2 to 0.8 mrad) $DDCS_{coh}$ drops below $DDCS_{inc}$ by up to a factor of 2, to once again become much larger than $DDCS_{inc}$ at θ $\gtrsim$ 0.9 mrad. Since all experimental conditions apart from L were kept identical for both data sets, these differences clearly demonstrate that L, and therefore the projectile coherence, has a major effect on the angular dependence of the DDCS.
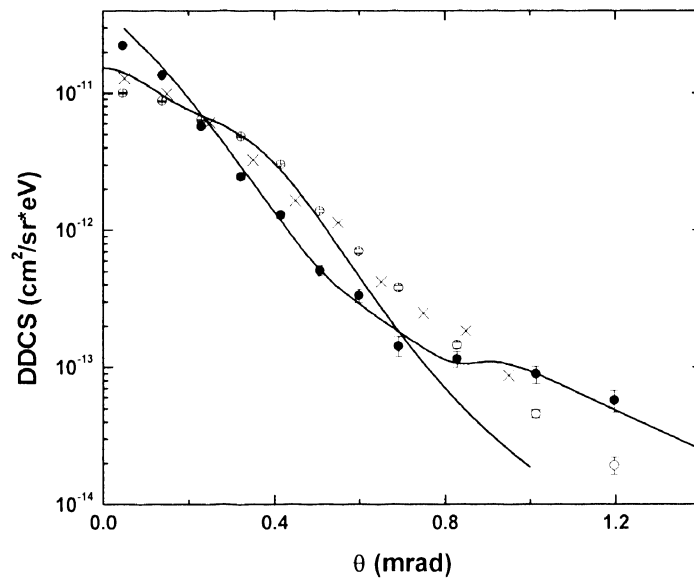
FIG.1. Double differential cross sections for ionization of H_2 by ion impact as a function of scattering angle for a projectile energy loss of 30 eV. The closed symbols show the data for a large slit-target distance L corresponding to a transverse coherence length Δr larger than the internuclear separation D, the open symbols show the data for small L corresponding to Δr < D. The crosses are data for ionization of atomic hydrogen [25,26]. The solid curve is a molecular 3-body distorted wave (M3DW) calculation [24], which assumes a completely coherent projectile beam. The dashed curve is a second Born approximation with Coulomb waves (SBA-C) calculation for ionization of atomic hydrogen [26,28].

The solid curve in figure. 1 shows a calculation based on the molecular 3-body distorted wave (M3DW) approach [24]. Like the experimental data, this calculation is averaged over all molecular orientations. Most importantly for the present context, the projectile is treated as fully coherent. This calculation reproduces the measured $DDCS_{coh}$ very well, but is in poor agreement with the $DDCS_{inc}$. At the same time, the shape of the angular distribution of the $DDCS_{inc}$ agrees nearly perfectly with the DDCS for atomic hydrogen ($DDCS_H$) measured earlier [25,26] and which are shown as crosses in Fig. 1. The $DDCS_H$ were multiplied by 2 to account for the presence of 2 electrons in H_2. (The data in Refs. [25,26] were not normalized to calculated $d\sigma/d(\Delta E)$ of Rudd et al., but to experimental values by Park et al. [27]. As a result, the $DDCS_H$ shown in Fig. 1 divided by 2 differ by about 25% from the data of Refs. [25,26].) The shape of the angular dependence of the $DDCS_{inc}$ is also well reproduced by $DDCS_H$ calculated using a modification of the second Born approximation, except for large θ (dashed curve in Fig.1). In this model, which was labeled SBA-C, the projectile is described by a Coulomb wave rather than a plane wave [26,28]. Although this also represents a fully coherent treatment of the projectile, its effect on the DDCS is strongly suppressed, if visible at all, compared to the molecular target. The interference for a molecular target is a particularly prominent manifestation of the projectile coherence, which is obviously not present for atomic hydrogen, even if the projectile beam is fully coherent. Furthermore, the ionization potentials of H and H_2 are very similar. Therefore, if $\Delta r < D$, i.e., if only one H atom in the molecule is illuminated at a time, the ionization process should basically behave like ionization of H and one would expect the $DDCS_{inc}$ to exhibit the same angular dependence as the $DDCS_H$, assuming that the projectile coherence has no

significant effect on the latter. That this is indeed observed supports the conclusion that, at the smaller slit-target distance, it is the incoherence of the projectile beam which makes the $DDCS_{inc}$ so different from the $DDCS_{coh}$.

In analogy to optical double slit interference, the $DDCS_{coh}$ can be expressed in terms of the $DDCS_{inc}$ multiplied by an interference term (IT); i.e., the interference term is given by the cross section ratio $R = DDCS_{coh}/DDCS_{inc}$. The phase difference φ between the projectile waves diffracted at the two centers is a function of θ, the molecular orientation δ, and D. In our experiment δ was not determined and the DDCS therefore have to be averaged over all δ. This averaging leads to a damping, but not to a complete elimination of the interference structure [26,28]. The measured ratio R, i.e., the interference term, is shown in Fig. 2 as a function of the scattering angle. A pronounced maximum can be seen at $\theta = 0$ and a minimum near $\theta = 0.5$ mrad. R then steeply rises again to approach a second interference maximum, which, however, lies only partly within the angular range covered in the experiment. The solid line shows the ratio between the $DDCS_{coh}$ calculated with the M3DW model (solid line in Fig. 1) and the $DDCS_{11}$ calculated with the SBA-C model (dashed line in Fig. 1). As mentioned above, the $DDCS_{11}$ should to a very good approximation exhibit the same θ dependence as the $DDCS_{inc}$; i.e., like the data this theoretical ratio should represent to a good approximation the interference term. These theoretical R are in excellent agreement with the measured values for scattering angles smaller than about 0.7 mrad, but they considerably overestimate the experimental R at larger θ. However, these discrepancies are not primarily due to an incorrect description of the interference, but mainly result from an underestimation of the experimental $DDCS_{11}$ at large θ (see Fig. 1).
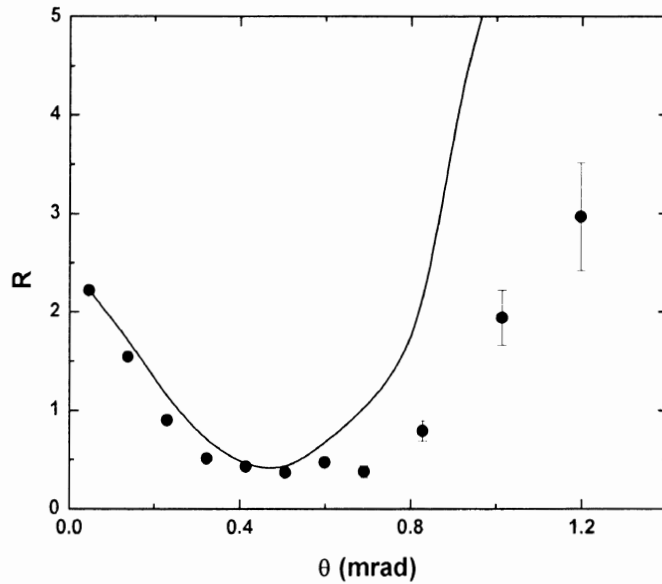
FIG. 2. Ratios between the double differential cross sections for ionization of H_2 for a large slit-target distance (closed symbols in Fig. 1) and for a small distance (open symbols in Fig. 1). The solid curve shows the ratio between the double differential cross sections calculated for ionization of H_2 using the M3DW model and for ionization of atomic hydrogen calculated using the SBA-C model.

Overall, the interpretation of the differences between $DDCS_{coh}$ and $DDCS_{inc}$ as due to the interference is qualitatively supported by the theoretical R.

In summary, an interference structure due to indistinguishable scattering of a proton beam from the two atomic centers of H_2 was observed if a collimating slit was placed at a large distance from the target, but not for a small distance. We do not consider the presence of interference effects per se to be the most significant result. Rather, we believe that the most important conclusion to be drawn from this work is that the preparation of the projectile beam affects the scattering cross sections, not because of imperfections in the experiment, but because of the fundamentals of quantum mechanics.

Many decades of atomic scattering theory are based on the assumption that the projectile beam is prepared coherently. In many cases (like, e.g., electron scattering or cross sections integrated over projectile parameters) this assumption may represent a very good approximation; however, it is not sustainable in general. Here, we presented an example, namely, incoherent proton scattering leading to ionization of H_2, where this assumption leads to qualitatively incorrect results.

Our results demonstrate that the projectile has to be described by a three-dimensionally localized wave packet with finite width. Collision systems involving atomic targets are potentially also significantly affected by the projectile coherence. For example, the long-standing puzzle regarding discrepancies between theory and experiment in the FDCS for ionization in 100 MeV/amu C^{6+} + He collisions [2] could probably be solved by properly accounting for the localization of the projectile. More specifically, the incorrect assumption of a fully coherent projectile beam probably leads to artificial path interference between two (or more) different impact parameters, resulting in the same scattering angle, in theory [29].

[1] E. Rutherford, Philos. Mag. **21**, 669 (1911).

[2] M. Schulz, R. Moshammer, D. Fischer, H. Kollmus, D. H.Madison, S. Jones, and J. Ullrich, Nature (London) **422**,48 (2003).

[3] T. N. Rescigno, M. Baertschy, W.A. Isaacs, and C.W. McCurdy, Science **286**, 2474 (1999).

[4] L. S. Rodberg and R. M. Thaler, Introduction to the Quantum Theory of Scattering (Academic Press, New York 1967).

[5] H. Bethe, Ann. Phys. (Leipzig) **397**, 325 (1930).

[6] E.Y. Kamber, C. L. Cocke, S. Cheng, and S. L. Varghese, Phys. Rev. Lett. **60**, 2026 (1988).

[7] R. Dörner, V. Mergel, R. Ali, U. Buck, C. L. Cocke, K. Froschauer, O. Jagutzki, S. Lencinas, W. E. Meyerhof, S. Nüttgens, R. E. Olson, H. Schmidt-Böcking, L. Spielberger, K. Tökesi, J. Ullrich, M. Unverzagt, and W. Wu, Phys. Rev. Lett. **72**, 3166 (1994).

[8] R. Moshammer, M. Unverzagt, W. Schmitt, J. Ullrich, and H. Schmidt-Böcking, Nucl. Instrum. Methods Phys. Res., Sect. B **108**, 425 (1996).

[9] N.V. Maydanyuk, A. Hasan, M. Foster, B. Tooke, E. Nanni, D. H. Madison, and M. Schulz, Phys. Rev. Lett. **94**, 243201 (2005).

[10] M. Schulz, Phys. Scr. **80**, 068101 (2009).

[11] M. Dürr, C. Dimopoulou, B. Najjari, A. Dorn, K. Bartschat, I. Bray, D.V. Fursa, Z. Chen, D. H. Madison, and J. Ullrich, Phys. Rev. A **77**, 032717 (2008).

[12] M. McGovern, C. T. Whelan, and H. R. J. Walters, Phys. Rev. A **82**, 032702 (2010).

[13] M. Schulz, M. Dürr, B. Najjari, R. Moshammer, and J.Ullrich, Phys. Rev. A **76**, 032712 (2007).

[14] H. Kaiser, S.A.Werner, and E. A. George, Phys. Rev. Lett.**50**, 560 (1983).

[15] A. D. Cronin, J. Schmiedmayer, and D. E. Pritchard, Rev. Mod. Phys. **81**, 1051 (2009).

[16] V. Kohn, I. Snigireva, and A. Snigirev, Phys. Rev. Lett. **85**, 2745 (2000).

[17] T. F. Tuan and E. Gerjuoy, Phys. Rev. **117**, 756 (1960).

[18] L. Ph. H. Schmidt, S. Schössler, F. Afaneh, M. Schöffler, K. E. Stiebing, H.

Schmidt-Böcking, and R. Dörner, Phys.Rev. Lett. **101**, 173202 (2008).

[19] J. S. Alexander, A. C. Laforge, A. Hasan, Z. S. Machavariani, M. F. Ciappina, R. D. Rivarola, D. H. Madison, and M. Schulz, Phys. Rev. A **78**, 060701(R) (2008).

[20] N. Stolterfoht, B. Sulik, V. Hoffmann, B. Skogvall, J.Y. Chesnel, J. Rangama, F. Frèmont, D. Hennecart, A. Cassimi, X. Husson, A. L. Landers, J. A. Tanis, M. E. Galassi, and R. D. Rivarola, Phys. Rev. Lett. **87**, 23201 (2001).

[21] D. Misra, U. Kadhane, Y. P. Singh, L. C. Tribedi, P. D. Fainstein, and P. Richard, Phys. Rev. Lett. **92**, 153201 (2004).

[22] M. Dürr, B. Najjari, M. Schulz, A. Dorn, R. Moshammer, A. B. Voitkiv, and J. Ullrich, Phys. Rev. A **75**, 062708 (2007).

[23] M. E. Rudd, Y.-K. Kim, D. H. Madison, and T. J. Gay, Rev. Mod. Phys. **64**, 441 (1992).

[24] J. Gao, J. L. Peacher, and D. H. Madison, J. Chem. Phys. **123**, 204302 (2005).

[25] A. C. Laforge, K. N. Egodapitiya, J. S. Alexander, A. Hasan, M. F. Ciappina, M. A. Khakoo, and M. Schulz, Phys. Rev. Lett. **103**, 053201 (2009).

[26] M. Schulz, A. C. Laforge, K. N. Egodapitiya, J. S. Alexander, A. Hasan, M. F. Ciappina, A. C. Roy, R. Dey, A. Samolov, and A. L. Godunov, Phys. Rev. A **81**, 052705 (2010).

[27] J. T. Park, J. E. Aldag, J. M. George, and J. L. Peacher, Phys. Rev. A **15**, 508 (1977).

[28] A. L. Godunov, V. A. Schipakov, and M. Schulz, J. Phys. B **31**, 4943 (1998).

[29] L. Sarkadi, Phys. Rev. A **82**, 052710 (2010).

2. Scattering-angle dependence of doubly differential cross sections for fragmentation of H_2 by proton impact

K.N. Egodapitiya, S. Sharma, A.C. Laforge*, and M. Schulz

Dept. of Physics and LAMOR, Missouri University of Science & Technology, Rolla, MO 65409, USA

We have measured double differential cross sections (DDCS) for proton fragment formation for fixed projectile energy losses as a function of projectile scattering angle in 75 keV p + H_2 collisions. An oscillating pattern was observed in the angular dependence of the DDCS with a frequency about twice as large as what we found earlier for nondissociative ionization. Possible origins for this frequency doubling are discussed.

I. INTRODUCTION

Collisions of charged particles with molecular hydrogen have been studied extensively over the last decade because H_2 represents the simplest target with multiple scattering centers (e.g., Refs. [1-14]). This property can give rise to various manifestations of quantum-mechanical interference in differential cross sections for ionization, electron capture, or other scattering processes. Already 50 years ago Tuan and Gerjuoy [15] presented a theoretical analysis of interference in the scattered projectile wave due to indistinguishable diffraction of the projectile from the two atomic centers in the molecule. But it was only more than 30 years later that interference effects were first reported in measured capture and ionization cross sections as a function of the molecular orientation [16].

The interest in molecular interference effects significantly intensified when they were observed in measured double differential cross sections as a function of the energy of electrons ejected from H_2 by highly charged ion impact (e.g., Refs. [1-3]). Here, the data were interpreted as interference in the ejected electron wave due to indistinguishable emission from the two atomic centers. However, the reported structures were not very pronounced; only after normalizing the data to calculations for atomic hydrogen was an oscillation observed. Significantly more pronounced interference structures were found in capture cross sections as a function of the molecular orientation in $He^{2+} + H_2$ collisions [9] and in fully differential recoil-ion momentum spectra for capture in $H_2^+ + He$ collisions [7]. In both cases the observed process did not involve any ejected electron and the interference can thus only originate from indistinguishable diffraction of the atomic

(or ionic) collision partner from the two atomic centers of the molecular collision partner, as originally described by Tuan and Gerjuoy [15].

Finally, interference structures were also observed in the double differential cross sections (DDCS) for fixed projectile energy loss ε as a function of projectile scattering angle θ for target ionization in $p + H_2$ collisions [8]. Here, generally both types of interferences, in the ejected electron wave and in the diffracted projectile wave, can contribute. However, in that experiment the kinematic conditions were chosen such that the magnitude of the momentum transfer $\mathbf{q}$ (defined as the difference between the initial and final projectile momentum) was for most of the angular range large compared to the ejected electron momentum. Therefore, the phase angle in the interference term was not affected much by the ejected electron.

The phase angle φ in the interference resulting from the diffracted projectile wave contains two components. One component is due to the difference in the total distance that the projectile waves from the two atomic centers propagate to the detector. Only the projection of the molecular orientation onto the transverse plane (i.e. perpendicular to the initial projectile beam axis) contributes to this component of the phase angle, which we call the geometric phase angle φ_{geo}. The second component results from the change in the projectile De Broglie wavelength λ due to the ejection of the electron. The phase angle depends on where, relative to the center of mass of the molecule, the energy loss of the projectile occurs. Only the projection of the molecular orientation onto the longitudinal axis contributes to this component of the phase angle, which we call the De Broglie phase angle φ_{dB}. It should be noted that φ_{dB} is independent of θ and thus cannot by itself lead to an oscillating pattern in the angular dependence of the DDCS. Furthermore, one would

expect the interference structure not to depend significantly on the ejected electron energy, which was indeed observed [8].

A switch of the symmetry between the initial and final electronic state can lead to a phase shift of π in the phase angle of the interference term [7]. Apart from such a phase jump one would expect that the interference structure in the DDCS originating in the diffracted projectile wave is to a large extent also independent of the process occurring in the collision if the momentum of any ejected electron is small compared to q. In this article we report measurements of DDCS for ionization accompanied by fragmentation (IF) of H_2 by 75 keV proton impact, which leads to at least one positively charged fragment. Several channels contribute to IF and most of them proceed through the two-electron processes of double excitation followed by auto-ionization, ionization-excitation, and double ionization [17,18]. The only one-electron process that can lead to IF is single ionization accompanied by vibrational excitation of the molecule [10,18]. The results are compared to DDCS, which we measured earlier for single (nondissociative) ionization for the same collision system [8].

II. EXPERIMENT

A schematic diagram of the experiment, which was performed at Missouri University of Science & Technology, is shown in Fig. 1. A proton beam with an energy spread of << 1 eV was produced with a hot cathode ion source and accelerated to an energy of 75 keV. The beam was collimated by a set of slits 0.15 mm x 0.15 mm in size located 50 cm before the target region. The projectile wave packet originating from the slit has a transverse width of about 2 a.u. for this geometry, which is larger than the inter-nuclear separation of the H_2 molecule of 1.4 a.u. We recently demonstrated that an
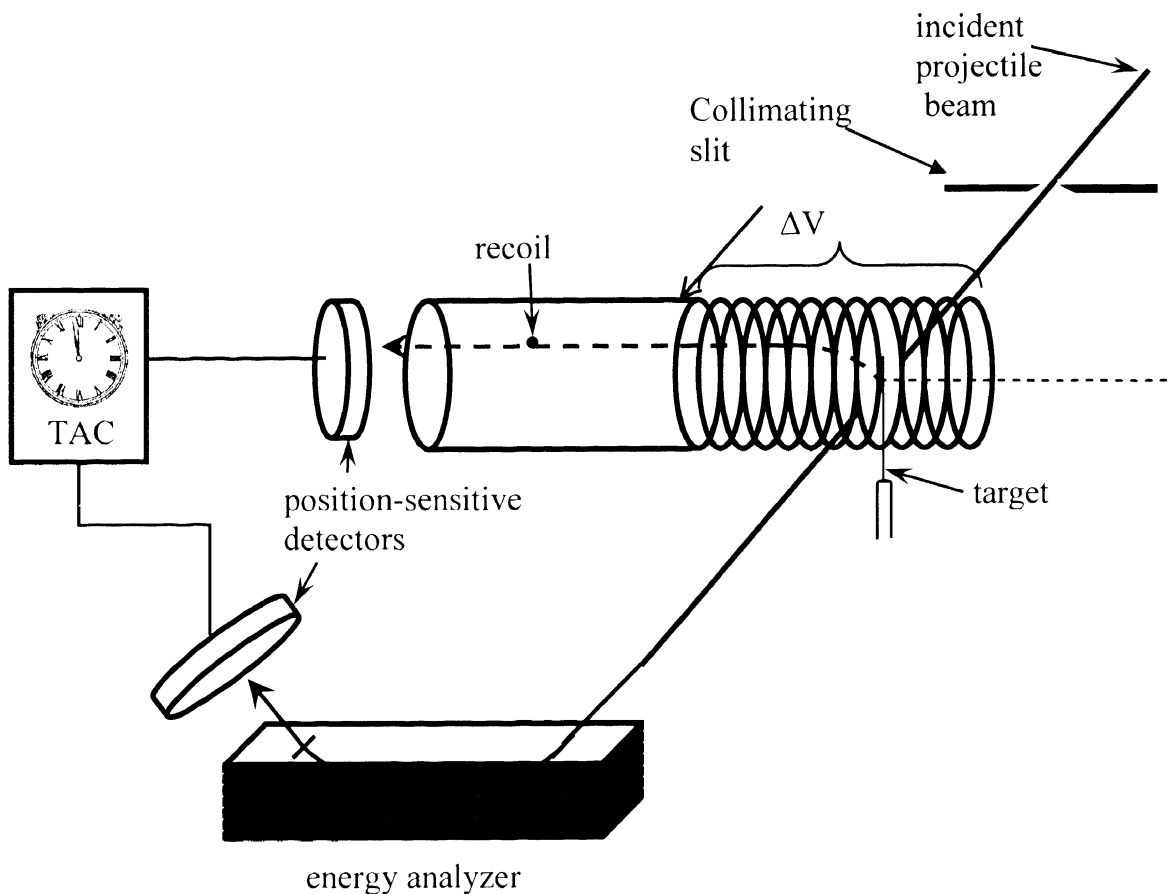
FIG. 1. Schematic diagram of the experimental setup.

interference in the projectile wave requires a coherent projectile beam (i.e., a width of the incoming projectile wave packet that is larger than the internuclear separation of the molecule). The protons were crossed with a molecular hydrogen beam produced by a supersonic jet.

The positively charged molecular fragments were extracted by an electric field of about 85 V/cm and guided onto a channel-plate detector. This relatively strong field was necessary to efficiently collect fragments for a broad range of momenta. At this field the size of the recoil-ion detector limited the momenta of the detected fragments to about 22

a.u. (corresponding to a kinetic energy of 3.6 eV) in the plane parallel to the detector surface.

After the collision, the projectile beam was charge-analyzed by a switching magnet (not shown in Fig. 1). The protons were decelerated by 70 keV, energy-analyzed by an electrostatic parallel plate analyzer [19], and detected by a two-dimensional position-sensitive channel-plate detector. Therefore, all scattering angles θ between 0 and approximately 2 mrad were recorded simultaneously in a single run. However, the very narrow entrance and exit slits of the energy analyzer restricted recording of data to only one projectile energy loss ε at a time. The resolution in ε was ± 1.5 eV and the resolution in θ was ± 0.05 mrad. The projectile and recoil-ion detectors were set in coincidence.

III. RESULTS AND DISCUSSION

In Fig. 2 a typical coincidence time spectrum is shown (recorded for $\varepsilon = 50$ eV). The time of flight of the projectile from the target region to the detector is practically constant because ε is very small compared to the initial projectile energy. Therefore, the coincidence time (i.e., the time difference between the timing of the recoil ion and projectile signal) reflects the time of flight recoil ions T_{rec}. Because T_{rec} is inversely proportional to the square root of the mass of the recoil ion, nondissociative ionization (NDI), leading to H_2^+ ions (approx. at channel 160), is separated in the time spectrum from IF leading to proton fragments (approx. at channel 135). The DDCS for IF (D_{IF}) could therefore be extracted by generating the projectile position spectrum with a condition on the proton peak in the time spectrum. The D_{IF} were normalized to the single differential cross section $d\sigma/d\varepsilon$, which, in turn, were obtained from the ratio of the
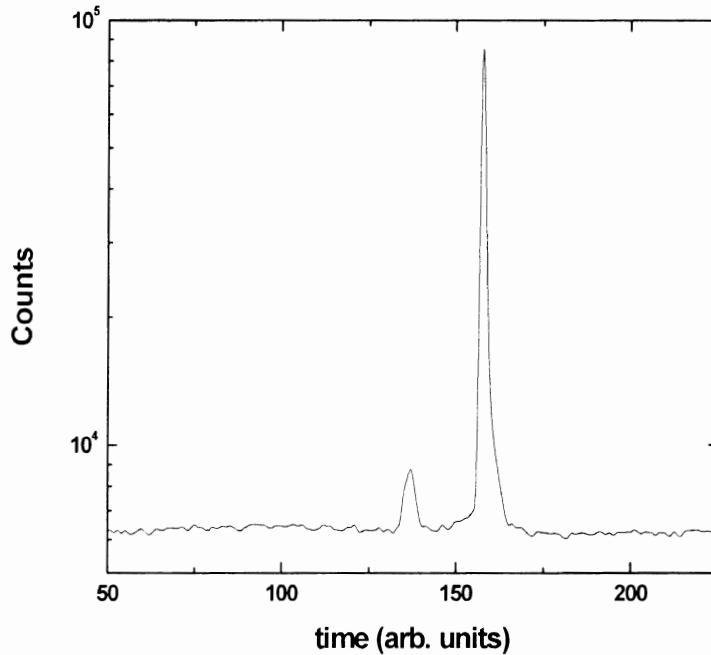
FIG. 2. Projectile–recoil-ion coincidence time spectrum. The peak structures near channels 135 and 160 represent proton fragment and H_2^+ formation, respectively.

integrated proton to H_2^+ time peaks multiplied by $d\sigma/d\varepsilon$ for NDI. The latter were calculated using the semiempirical model proposed by Rudd et al. [20], which has been very successful in reproducing measured values.

The measured D_{IF} are shown in Fig. 3 as a function of θ for $\varepsilon = 27$ (top left), 30 (top right), 40 (bottom left), and 50 eV (bottom right). The cross sections fall off rapidly with increasing θ; however, apart from this trend weak maxima can be seen for all ε at the same angle of about 1.2 mrad. At first glance the shape of the D_{IF} looks quite similar to what we observed earlier for NDI [8] for the same collision system. For comparison, these latter data are shown in the top panels of Fig. 4 for $\varepsilon = 30$ eV (left) an $\varepsilon = 50$ eV (right). However, a closer inspection of the D_{IF} reveals some differences to D_{NDI}. An

additional structure can be seen at a scattering angle around 0.6 to 0.7 mrad. This structure is not very pronounced, but it systematically occurs for all ε at the same angle and can thus not be discarded.

The structures near 0.6-0.7 mrad are much more prominent in the ratios R between the D_{IF} and twice the DDCS for single ionization of atomic hydrogen (D_{II}), which are plotted in Fig. 5.

FIG. 3. Double differential cross sections (DDCS) for proton fragment formation plotted as a function of the projectile scattering angle θ for fixed energy losses ε of 27 (top left), 30 (top right), 40 (bottom left), and 50 eV (bottom right), respectively.

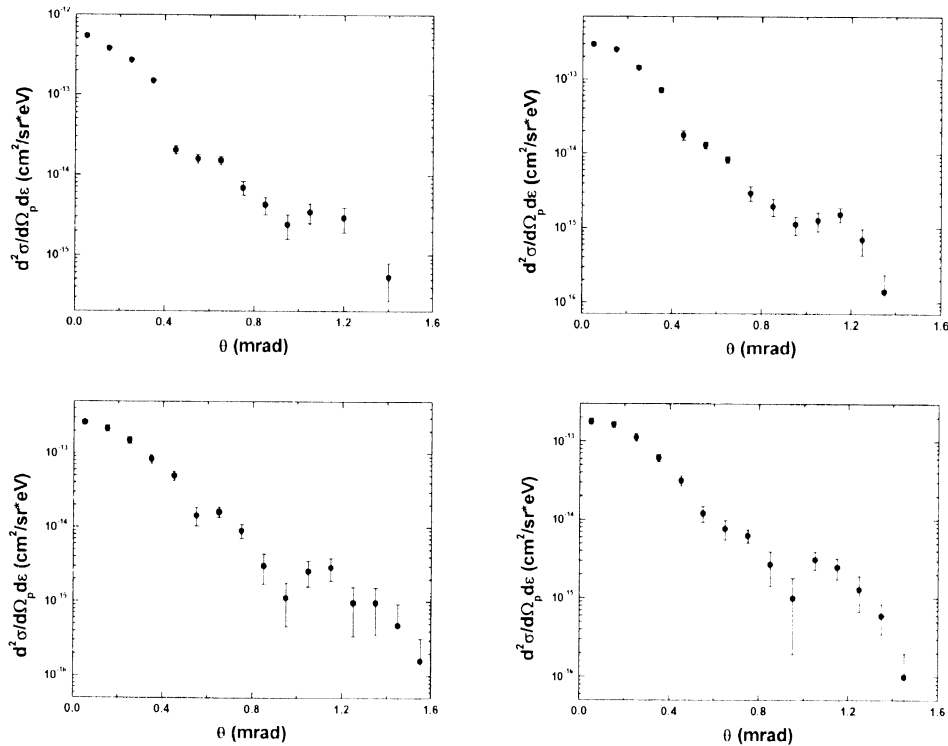Experimental data for the latter [21,22] were well reproduced by a Second Born

Approximation with Coulomb waves (SBA-C) at small and intermediate θ and by a

continuum-distorted-wave–eikonal-initial-state (CDW-EIS) calculation at large θ [22].

We therefore combined these two calculations to obtain an essentially perfect fit to the

experimental data by which we divided the measured D_{IF} to compute R. The same fit

was also used to generate the corresponding ratios for NDI, which are shown in the

bottom panels of Fig. 4 for $\varepsilon = 30$ eV (left) and $\varepsilon = 50$ eV (right)[1]. In the case of IF 3

maxima are observed in R at almost identical angles of about 0.2, 0.7, and 1.2 mrad for

all ε. In the ratios for NDI, structures are seen near angles of 0.2 and 1.2 mrad as well;

however, no maximum is discernable near 0.7 mrad.

In the case of NDI the interference term T_{IT} can to a good approximation be

represented as the ratio between the D_{NDI} and the incoherent part of the cross sections

D_{inc} [8]. Therefore, making the assumption that D_{inc} is twice the DDCS for atomic

hydrogen, R_{NDI} is identical to T_{IT}. For a fixed molecular orientation T_{IT} is given by

$$T_{IT} = R_{NDI} = 1 + \cos(\mathbf{p_{rec}} \cdot \mathbf{D}) \tag{1}$$

where $\mathbf{p_{rec}}$ is the recoil-ion momentum vector (in the case of fragmentation it is the sum

momentum of both fragments) and $\mathbf{D}$ is the position vector of one atomic center of the

molecule relative to the other. If the molecular orientation is not fixed in the experiment

and assuming that all orientations contribute equally, the averaged interference term is [1]

---

[1] In the original publication of the NDI data [9] the DDCS were normalized to the CDW-EIS calculation for H.

$$T_{IT} = RNDI = 1 + \sin(p_{rec}D)/(p_{rec}D) \tag{2}$$

However, for IF it is not as straightforward to associate the ratios R_{IF} with the interference term because apart from the ionization of one electron it requires either a transition of the second electron or vibrational excitation of the molecule to a dissociative state. Using the approximation that this second step of IF is uncorrelated with the ionization of the first electron, R_{IF} can be expressed as

$$R_{IF} = D_{IF}/(2D_H) = D_{NDI}P_f/(2D_H) \tag{3}$$

where P_f is the probability for the second step of IF. If we further assume that the interference term is indeed, as argued earlier, to a large extent independent of the specific process occurring in the collision, we obtain $R_{IF} = T_{IT}P_f$, where T_{IT} is the same interference term as in NDI. The differences in R between NDI and IF would then simply reflect the θ dependence of P_f. Another possibility is that these differences are already inherent in the interference term. In that case the observed doubling in the frequency of the interference oscillation in IF compared to NDI would suggest a much larger phase difference between the waves diffracted from the two atomic centers. Finally, it is conceivable that the interference term does not only differ in the phase angle, but its general form could be substantially altered compared to NDI. In the following we will analyze the data for specific ε in order to address these possible causes for the frequency doubling in more detail.
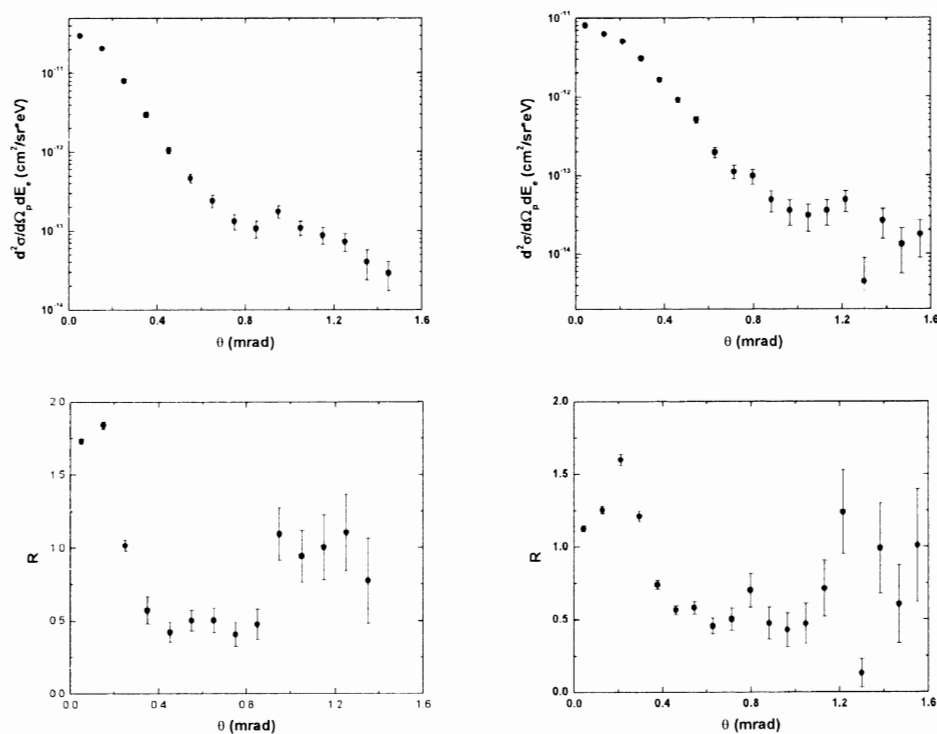
FIG. 4. DDCS for nondissociative ionization (NDI) plotted in the top panels as a function of the projectile scattering angle θ for fixed energy losses ε of 30 and 50 eV, respectively. The bottom panels show the ratios between the DDCS for NDI and twice the DDCS for single ionization of atomic hydrogen for the same energy losses.

As mentioned earlier, several processes contribute to the formation of proton fragments: single ionization accompanied by vibrational dissociation (also called ground state dissociation GSD [10]), double excitation followed by autoionization (DE), ionization plus excitation (IE), and double ionization (DI). The threshold energies for these processes are (in the same order) 18, 24, 31, and 48 eV for the outer turning point of the vibrational ground state (based on potential energy curves from Sharp [23] and Guberman [24]). Thus, at $\varepsilon = 27$ eV only GSD and DE can contribute to the measured D_{IF}. Experimental cross sections for these processes at the projectile energy studied here

are, to the best of our knowledge, not available. However, based on DE data for p + He collisions at similar projectile energies [25,26] we have to assume that DE is quite sizeable relative to NDI in the energy-loss region where DE occurs. On the other hand, only some doubly excited states are accessible at ε =27 eV and this energy loss is only 3 eV above the threshold for the lowest lying state ($^1\Sigma_g^+$). Furthermore, even this state can only be populated near the outer turning point. The Franck-Condon regime for transitions from the electronic and vibrational ground state covers internuclear distances from about D = 1.2 a.u.-1.7 a.u., but at ε = 27 eV DE is energetically possible only for D > 1.5 a.u.. Finally, for GSD, kinetic energy releases (KER) per fragment of more than 1 eV are entirely negligible [18] so that for this process all proton fragments are guided onto the recoil-ion detector. In contrast, for DE the KER spectrum at ε = 27 eV extends out to energies of about 4.5 eV per fragment so that here not all fragmentation events are detected. Therefore, the fraction of the D_{IF} due to GSD could be important as well. The total cross section ratio between GSD and NDI for fast proton impact is expected to be approximately 1.5% independent of the projectile velocity [27]. Our measured ratio between the single differential cross sections $d\sigma/d\varepsilon$ for IF and NDI is about 2.2%. We therefore crudely estimate that GSD contributes about 2/3 and DE 1/3 of the D_{IF} at ε =27 eV.

At ε = 30 eV, GSD and DE seem to contribute approximately equally to fragmentation. At ε = 40 eV DE is energetically no longer accessible in the Franck-Condon region for most doubly excited states. Therefore, at this energy loss only GSD
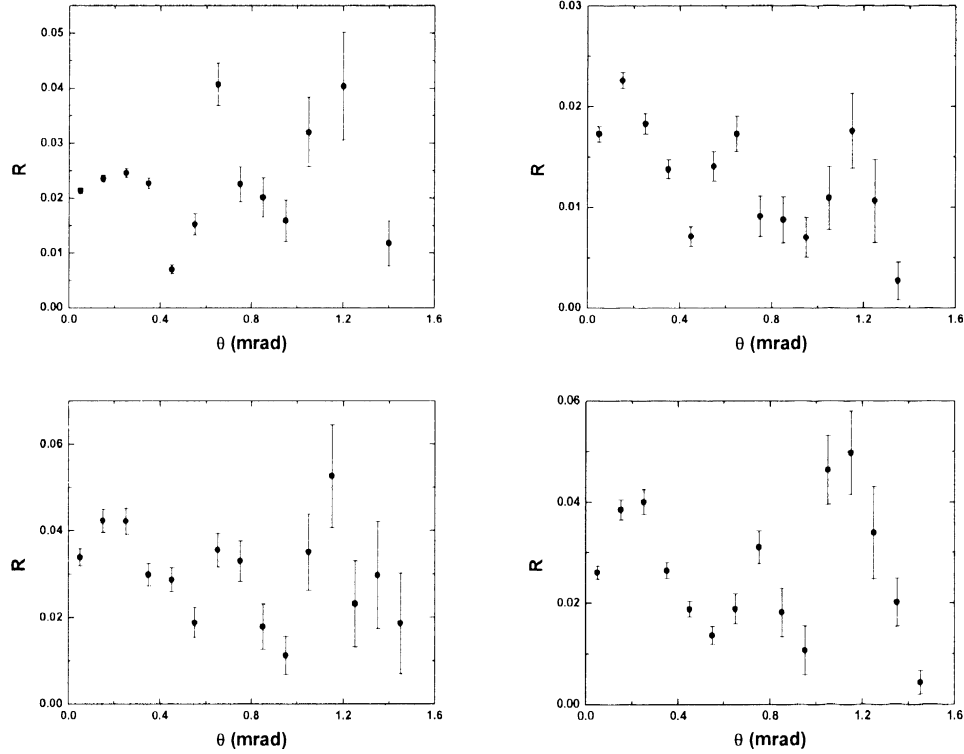
FIG. 5. Ratios between the measured DDCS for proton fragment formation of Fig. 3 and twice the DDCS for atomic hydrogen as a function of scattering angle for the same energy losses as in Fig. 3.

and IE contribute to formation of proton fragments. Finally, $\varepsilon = 50$ eV is just barely above the threshold for DI so that here, too, IF is dominated by GSD and IE. Furthermore, it should be noted that for IE the KER per fragment spectrum covers a range between 3 eV and 13 eV and for DI between 7 eV and 14 eV [20]. Therefore, most fragments produced by IE and all fragments produced by DI will not be detected if the molecule is oriented in the plane of the recoil-ion detector surface because of the limited momentum acceptance mentioned earlier.

In Fig. 6 we present $P_f = D_{IF}/D_{NDI}$ as a function of scattering angle for $\varepsilon = 27$ eV. These ratios exhibit essentially the same oscillatory pattern as R_{IF}. We therefore do not

believe that the differences in R between IF and NDI can be explained by the θ dependence of P_f, at least not under the assumption that IF can be viewed as a combination of two (or more) independent processes.

Next, we consider the possibility that the doubling of the interference frequency may be caused by a larger phase angle in IF compared to NDI. As mentioned earlier, for NDI and for a fixed molecular orientation the phase angle is given by $\varphi = \mathbf{p_{rec}} \cdot \mathbf{D}$. For our kinematics the electron momentum is small compared to q for most scattering angles so that to a good approximation $\varphi = q \, D \cos \alpha$, where α is the angle enclose by $\mathbf{q}$ and $\mathbf{D}$. Therefore, φ and thereby the oscillation frequency maximize when the molecule is aligned along the momentum transfer vector and for $D = 1.7$ a.u., which is the largest internuclear separation within the Franck-Condon region. It should be noted that GSD actually is more likely to take place near the inner turning point. But even for this maximized φ the oscillation frequency of the interference term is about a factor of 2 smaller than what we observe in the experiment.

The inability of Eq. (1) to reproduce the doubling of the interference frequency observed for GSD compared to NDI even under most favorable assumptions raises the question whether this form of T_{IF} is valid for GSD. Strong indications that this may not be the case were reported by Senftleben et al. [10], who measured fully differential cross sections (FDCS) for fixed molecular orientation for the same process for electron impact. For kinematic conditions which roughly correspond to $\theta \approx 0.7$ mrad in our data they observed constructive interference if the molecule was oriented parallel to $\mathbf{q}$ and
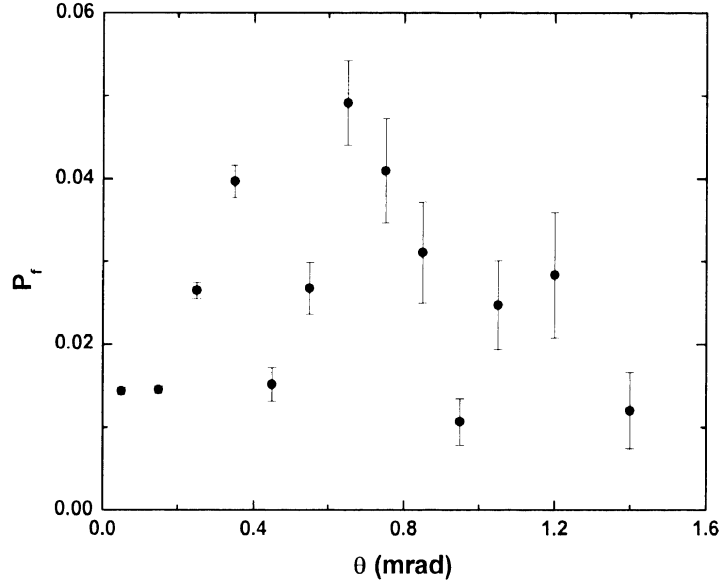
FIG. 6. Ratios P_f between the measured DDCS for proton fragment and H_2^+ formation as a function of scattering angle for $\varepsilon = 27$ eV.

destructive interference if it was oriented perpendicular to **q**. In contrast, the T_{IT} based on Eq. (1) predicts destructive interference for the parallel orientation and constructive interference for the perpendicular orientation. On the other hand, the molecular 3-body distorted wave (M3DW) approach [28], which is not based on equation (1), qualitatively reproduced the data of Senftleben et al. These observations correspond with the behavior of our D_{II} data around 0.6 to 0.7 mrad: Here, too, we observe constructive interference while in the corresponding data for NDI, which were found to be consistent with Eq. (1), destructive interference was observed in the same angular range [8]. The conclusion of Senftleben et al. that the interference of Eq. (1) is not applicable to GSD is thus not inconsistent with the present data.
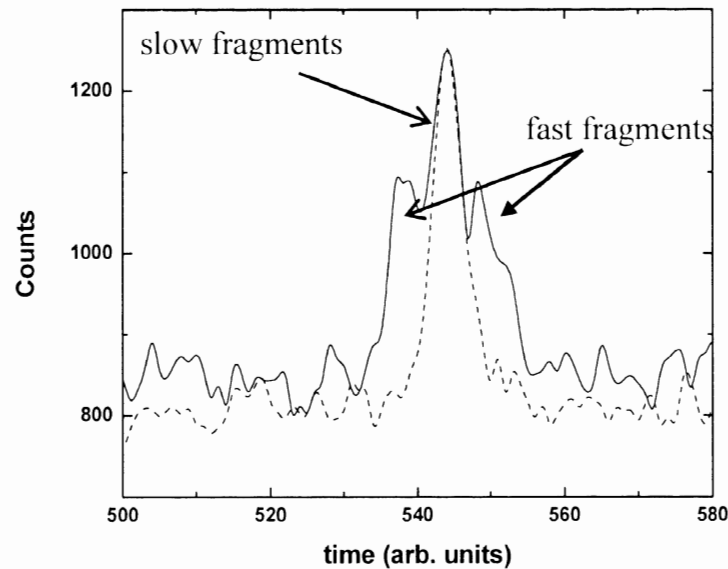
FIG. 7. Projectile–recoil-ion coincidence time spectrum for $\varepsilon = 30$ eV (dashed curve) and $\varepsilon = 50$ eV (solid curve) expanded over the region of the proton fragment peak. The resolution is improved compared to the time spectrum of Fig. 2 because the latter is compressed by a factor of 4.

The observation that R_{IF} hardly differs at all for the larger energy losses from $\varepsilon = 27$ eV suggests that if Eq. (1) indeed does not hold for GSD, this may also be true for proton fragment production through DE, IE, or DI. For $\varepsilon = 30$ eV, although DE is likely an important channel, we cannot entirely rule out that IF is dominated by GSD. However, a closer inspection of the coincidence time spectra leaves no doubt that for $\varepsilon = 40$ and 50 eV at least IE plays an important role. In Fig. 7 the proton time peak is expanded and plotted in higher resolution than in Fig. 2, which shows the time spectrum compressed by a factor of 4. The dashed and solid curves represent the time spectra for $\varepsilon = 30$ and 50 eV, respectively. These plots reveal that for $\varepsilon = 50$ eV the fragmentation leads to a triple peak, but at $\varepsilon = 30$ eV we only observe a single peak. The spectra for $\varepsilon = 27$ and 40 eV

are practically identical to those for ε = 30 and 50 eV, respectively. The side peaks at the larger energy losses represent fragments that are ejected with large momentum towards (left peak) or away from (right peak) the recoil-ion detector. Since for GSD, KER values larger than approximately 1 eV are entirely negligible and DE is no longer accessible for most states at energy losses of 40 eV and above, these contributions must come from IE. At ε =50 eV a small fraction from DI may also be present.

The center peak contains two components, one from GSD and one from IE and DI leading to fragments with small momenta in the direction of the extraction field (i.e., perpendicular to the plane of the detector). Since the KER spectra for these latter two processes only start at about 3 eV/fragment and the average energy is about 7 eV for IE and 9.5 eV for DI such events only contribute to the center peak if the molecule was oriented at some minimal angle relative to the extraction field. However, that angle cannot be too large either, because otherwise the fragments would not be detected due to the limited momentum acceptance of the detector. One would therefore expect such events to contribute to the regions in between the center and side peaks. The fact that these structures are separated from each other by minima suggests that the center peak is dominated by GSD. This is also supported by the observation that the ratio between the time peak contents for the slow p fragments and the H_2^+ ions of about 1.3% is very close to the expected ratio between the total cross sections for GSD and NDI (see the preceding discussion).

In the top panels of Fig. 8 we show the D_{IF} with an additional condition on the time peak for the slow fragments (closed symbols) and for the fast fragments (open symbols) for ε = 40 eV (left panel) and for ε = 50 eV (right panel). The data for the fast

fragments should be viewed as triple differential cross sections TDCS = $d^3\sigma/(d\Omega_p d\varepsilon d\Omega_m)$

for IE (and possibly a small component of DI for ε = 50 eV, which we neglect in the

following), because the molecular orientation is now determined
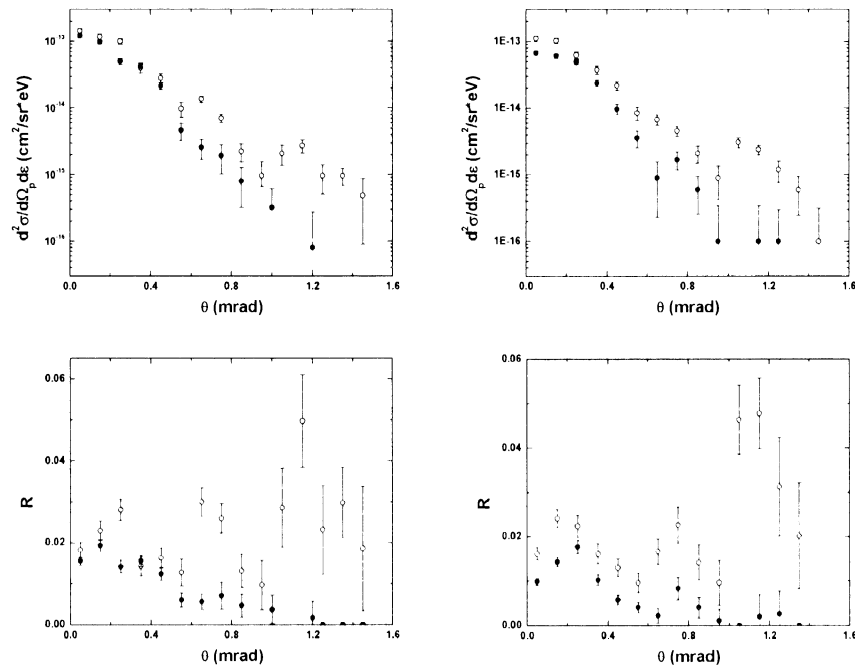
FIG. 8. DDCS for proton fragment formation plotted in the top panels as a function of
the projectile scattering angle θ for fixed energy losses ε of 40 and 50 eV, respectively,
with additional conditions on the time peak labeled "slow fragments" (closed symbols)
and "fast fragments" (open symbols) in Fig. 7. The bottom panels show the
corresponding ratios between these DDCS and twice the DDCS for single ionization of
atomic hydrogen.

However, the TDCS are not properly normalized, since we do not know the effective

solid angle for the detection of the molecular fragments. In contrast, the data for the slow

fragments still represent DDCS for GSD (neglecting possible contributions from IE and

DI), since they contain all molecular orientations due to the very small KER resulting

from this process.

The TDCS for IE look very similar to the D_{IF} without the condition on the proton time peak for both energy losses. The ratios between these TDCS and twice the D_H, plotted in the bottom panels of Fig. 8, show that the interference structure still exhibits a doubling of the oscillation frequency compared to the data for NDI. In contrast, the interference structure in the D_{IF} for GSD is strongly suppressed. Only the first maximum around 0.2 mrad is still visible in the ratios (at least at $\varepsilon = 50$ eV). But the two maxima at the larger scattering angles are completely absent, except, perhaps, for a trace of a maximum near 0.7 mrad for $\varepsilon = 50$ eV. Therefore, while for IE we find a similar behavior as for NDI in so far as the structures in the θ dependence of the cross sections do not depend very sensitively on the energy loss, the data for GSD are much more affected by ε.

We also observed a strong suppression of the interference structure at large ε for NDI [8]. However, there this effect only occurred around energy losses corresponding to ejected electron speeds v_{el} equal to the projectile speed v_p (i.e. for $\varepsilon \approx 56$ eV). In that work we therefore considered the possibility that the suppression of the interference structure may be correlated with the postcollision interaction (PCI) between the outgoing projectile and the ejected electron, which is known to maximize at the matching velocity $v_{el} = v_p$ [29,30]. Such a correlation is not confirmed by the present data for GSD because the interference structures are essentially absent already at $\varepsilon = 40$ eV, while the matching velocity corresponds to $\varepsilon = 59$ eV. A possible alternative explanation is based on the molecular orientation. If the molecule was always oriented along the projectile beam axis, the phase angle φ would not depend on θ. For NDI we found that the molecular orientation itself depended on θ favoring longitudinal (i.e. parallel to the projectile beam)

orientations at large θ and transverse orientations at intermediate θ. If the orientation remained fixed along the longitudinal direction over an extended range of scattering angles, no interference oscillation would be present in that range, while such structure could still occur at other θ. We therefore consider the possibility that GSD favors longitudinal molecular orientations over a much larger angular range than in NDI, possibly down to scattering angles as small as approximately 0.5 mrad (or smaller). One could then understand why the peak structures at 0.7 and 1.2 mrad, observed for $\varepsilon = 27$ and 30 eV, essentially disappear at larger ε, but that the maximum near 0.2 mrad nevertheless survives. However, at present we cannot offer an explanation why GSD would favor longitudinal orientations more than NDI does.

An alternative explanation for the doubling of the oscillation frequency emerges if causes for the structures other than molecular interference are considered. In the differential cross sections for DE in p + He collisions, as well as in the ratio to differential single excitation cross sections, a maximum was observed at around 0.7 mrad [25,26] (i.e. at roughly the same angle at which the second oscillation maximum occurs in the present data). Similar structures were also observed in corresponding ratios for other two-electron processes, e.g. DI [31], transfer ionization [32,33], or double capture [34] at about the same angle (except for DI). They were interpreted as due to interference between first- and higher-order transition amplitudes. For DE these structures were not observed for projectile energies below 150 keV. However, it should be noted that for H_2 the excitation energy is about a factor of 2 smaller than for He. Therefore, the projectile energy relative to the excitation energy in the present case is comparable to the DE studies for p + He collisions. It is reasonable to assume that such structures exist for IE as

well, although these ratios have not been measured yet for this process. The oscillations in the present data could then be explained by a combination of two independent components: (i) interference due to diffraction from the two atomic centers of the molecule, leading to the maxima near 0.2 and 1.2 mrad, and (ii) interference between first- and higher-order transition amplitudes leading to the maxima around 0.7 mrad.

IV. CONCLUSIONS

We have measured double differential cross sections (DDCS) for fragmentation of H_2 leading to at least one proton by 75 keV p impact for fixed energy losses ε as a function of scattering angle θ. In the θ dependence we observed an oscillating pattern for all ε. Several processes contribute to proton fragment formation. Ionization accompanied by vibrational dissociation and/or double excitation are the dominant channels at small ε and ionization plus excitation at large ε. Nevertheless, the data for different ε are very similar to each other, but, surprisingly, the frequency of the oscillation is about twice as large as what was observed for nondissociative ionization (NDI) for the same collision system [8].

At this time we cannot conclusively trace the origin of the frequency doubling compared to NDI. However, two possible alternative explanations emerge from the data analysis: First, the interference term that qualitatively describes various data sets for NDI (e.g., Refs. [1–6,8]) may not be applicable if ionization is accompanied by fragmentation of the molecule. Indications that this may be the case were reported earlier [10]. Second, the oscillation may be due to a combination of interference between the projectile waves diffracted at the two atomic centers of the molecule and interference between first and

higher-order amplitudes for the involved two-electron processes. We are currently preparing experiments, in which the kinetic energy release in the fragmentation will be measured. It will then be possible to isolate ionization accompanied by vibrational dissociation from the two-electron processes. A persistence of the frequency doubling would indicate that the interference term for the fragmentation process indeed has a different form than for NDI. On the other hand, a frequency similar to what is observed for NDI would suggest that the frequency doubling is characteristic of two-electron processes. Interference between first- and higher-order scattering amplitudes would then represent a plausible explanation.

ACKNOWLEDGMENTS

[1] N. Stolterfoht et al., Phys. Rev. Lett. **87** 23201 (2001).

[2] N. Stolterfoht et al., Phys. Rev. A **67**, 030702 (2003)

[3] D. Misra, U. Kadhane, Y. P. Singh, L. C. Tribedi, P. D. Fainstein, and P. Richard Phys. Rev. Lett. **92**, 153201 (2004)

[4] D. S. Milne-Brownlie, M. Foster, Junfang Gao, B. Lohmann, and D. H. Madison, Phys. Rev. Lett. **96**, 233201 (2006)

[5] D. Misra, A. Kelkar, U. Kadhane, Ajay Kumar, Lokesh C. Tribedi, and P. D. Fainstein Phys. Rev. A **74**, 060701 (R) (2006)

[6] E.M. Staicu Casagrande et al., I. Bray, J. Phys. B **41**, 025204 (2008)

[7] L. Ph. H. Schmidt, S. Schössler, F. Afaneh, M. Schöffler, K. E. Stiebing, H. Schmidt-Böcking, and R. Dörner, Phys. Rev. Lett. **101**, 173202 (2008)

[8] J.S. Alexander, A.C. Laforge, A. Hasan, Z.S. Machavariani, M.F. Ciappina, R.D. Rivarola, D.H. Madison, and M. Schulz, Phys. Rev. **A78**, 060701(R) (2008)

[9] D. Misra et al., Phys. Rev. Lett. **102**, 153201 (2009)

[10] A. Senftleben, T. Pflüger, X. Ren, O. Al-Hagan, B. Najjari, D.H. Madison, A. Dorn, J. Ullrich, J. Phys. B **43**, 081002 (2010)

[11] C. R. Stia, O. A. Fojón, P. F. Weck, J. Hanssen, B. Joulakian, and R. D. Rivarola Phys. Rev. A **66**, 052709 (2002)

[12] M. E. Galassi, R. D. Rivarola, and P. D. Fainstein, Phys. Rev. A **70**, 032721 (2004)

[13] M. F. Ciappina and R. D. Rivarola, J. Phys. B **41** 015203 (2008)

[14] J. Colgan, O. Al-Hagan, D.H. Madison, C. Kaiser, A.J. Murray, M.S. Pindzola, Phys. Rev. A **79**, 052704 (2009)

[15] T. F. Tuan and E. Gerjuoy, Phys. Rev. **117**, 756 (1960)

[16] S. Cheng, C. L. Cocke, V. Frohne, E. Y. Kamber, J. H. McGuire, and Y. Wang, Phys. Rev. A **47**, 3923 (1993)

[17] A. K. Edwards, R. M. Wood, A. S. Beard, and R. L. Ezell, Phys. Rev. A **37**, 3697 (1988)

[18] A. K. Edwards, R. M. Wood, J.L. Davis, and R. L. Ezell, Phys. Rev. A **42**, 1367 (1990)

[19] A.D. Gaus, W. T. Htwe, J. A. Brand, T. J. Gay, and M. Schulz, Rev. Sci. Instrum. **65** 3739 (1994)

[20] M.E. Rudd, Y.-K. Kim, D.H. Madison, and T.J. Gay, Rev. Mod. Phys. **64**, 441 (1992)

[21] A.C. Laforge, K.N. Egodapitiya, J.S. Alexander, A. Hasan, M.F. Ciappina, M.A. Khakoo, and M. Schulz, Phys. Rev. Lett. **103**, 053201 (2009)

[22] M. Schulz, A.C. Laforge, K.N. Egodapitiya, J.S. Alexander, A. Hasan, M.F. Ciappina, A.C. Roy, R. Dey, A. Samolov, and A.L. Godunov, Phys. Rev. A **81**, 052705 (2010)

[23] T.E. Sharp, At. Data **2**, 119 (1971)

[24] S.L. Guberman, J. Chem. Phys. **78**, 1404 (1983)

[25] W.T. Htwe, T. Vajnai, M. Barnhart, A.D. Gaus, and M. Schulz, Phys. Rev. Lett. **73**, 1348 (1994)

[26] M. Schulz, W.T. Htwe, A.D. Gaus, J.L. Peacher, and T. Vajnai, Phys. Rev. A **51**, 2140 (1995)

[27] I. Ben-Itzhak, V. Krishnamurthi, K.D. Carney, H. Aliabadi, H. Knudsen, U. Mikkelsen, and B.D. Esry, J. Phys. B **29**, L21 (1996)

[28] J. Gao, J. L. Peacher, and D. H. Madison, J. Chem. Phys. **123**, 204302 (2005)

[29] T. Vajnai, A.D. Gaus, J.A. Brand, W. Htwe, D.H. Madison, R.E. Olson, J.L. Peacher, and M. Schulz, Phys. Rev. Lett. **74**, 3588 (1995)

[30] M. Schulz, T. Vajnai, A.D. Gaus, W. Htwe, D.H. Madison, and R.E. Olson, Phys. Rev. A **54**, 2951 (1996)

[31] J. P. Giese and E. Horsdal, Phys. Rev. Lett. **60**, 2018 (1988)

[32] E. Horsdal, B. Jensen, and K. O. Nielsen, Phys. Rev. Lett. **57**, 1414 (1986)

[33] S.W. Bross, S.M. Bonham, A.D. Gaus, J.L. Peacher, T. Vajnai, H. Schmidt-Böcking, and M. Schulz, Phys. Rev. A **50**, 337 (1994)

[34] M. Schulz, T. Vajnai, and J.A. Brand, Phys. Rev. A **75**, 022717 (2007)

2. UNPUBLISHED DATA

Paper I described an experiment which investigated the effect of the projectile

coherence on the measured double differential cross sections for ionization of H_2. To

investigate similar effects for other processes, an experiment was performed to measure

the single differential cross sections (SDCS) as a function of the projectile scattering

angle for 75 keV proton impact on H_2 and 25 keV proton impact on H_2 and He. Here too,

as in the ionization case described in Paper I, measurements were done for two different
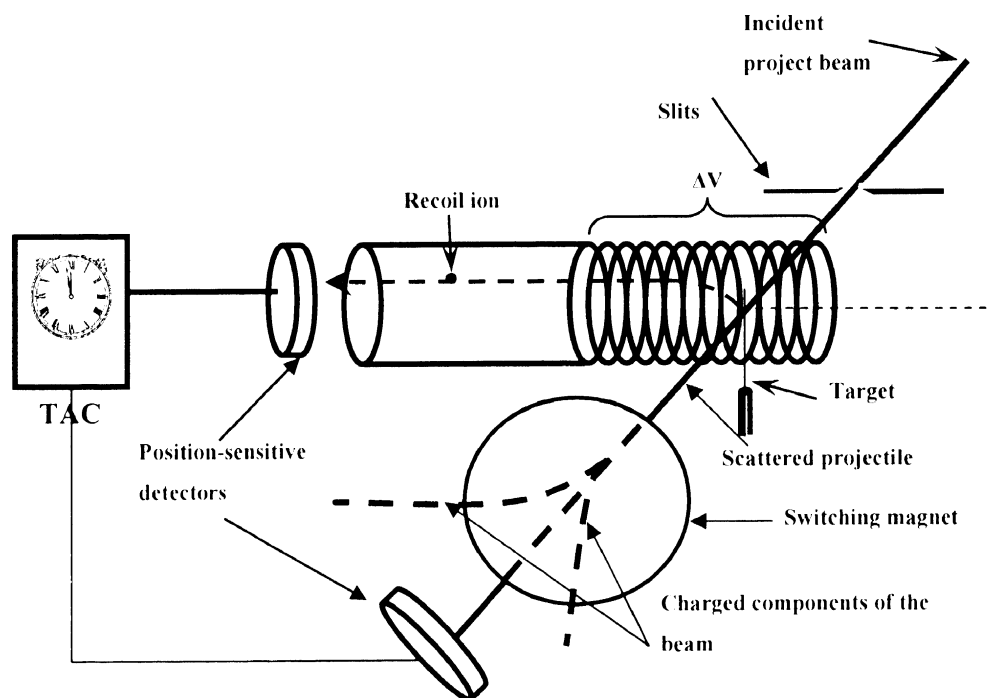
target-slit distances.

Figure 2.1 Experimental set up for single electron capture by 75 keV and 25 keV proton impact

However, in contrast to the experiment described in paper I, in this experiment, measurements for the two distances were carried out simultaneously.

Figure 3.1 shows a schematic diagram of the experimental set up. A beam of protons with 75 keV (or 25 keV) energy are collimated by two slits of width 0.15 mm. Here the x-slit was placed at a distance 6.5 cm away from the target. As mentioned in paper I, for this distance the projectile beam is incoherent. The y-slit was placed 50 cm away from the target and in this direction the projectile beam is coherent. The recoil ions were extracted by a small electric filed (≈ 2V/cm) and were detected by a position sensitive detector. The scattered projectiles were charge-separated by a switching magnet, and therefore only the neutral beam traveled along its initial path, after the collision.
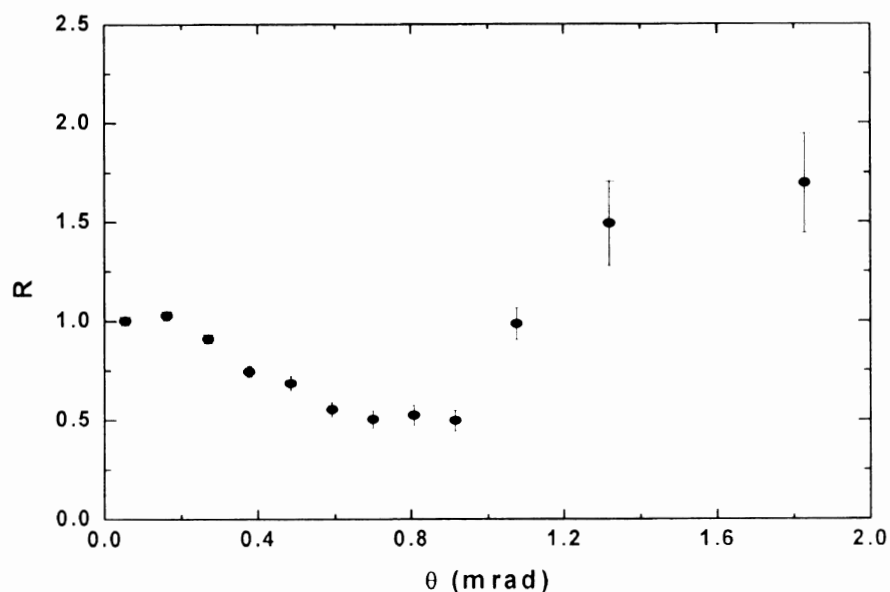

Figure 2.2 The ratio R= $SDCS_{coh}/SDCS_{incoh}$ for single electron capture by 75 keV p +H_2.

This neutral beam was detected by another two-dimensional position sensitive detector. The two detectors were set in coincidence. All the scattering angles between 0 and approximately 2.0 mrad were recorded simultaneously. Since the projectile beam is coherent in the y-direction and incoherent in the x-direction, the ratio of the SDCS in the y-direction ($SDCS_{coh}$) to SDCS in the x-direction ($SDCS_{inc}$) will give the interference term (see paper I).

As mentioned earlier, in the coherent case, the width of a projectile wave packet is larger than the inter-nuclear separation in the H_2 molecule. Therefore both atomic centers will be illuminated simultaneously which can lead to an interference pattern. On the other hand in the incoherent case, since the width of the projectile wave packet is smaller than the inter-nuclear separation in H_2, only one atom will be illuminated at a time therefore an interference structure will not be present. Figure 3.2 shows the ratio R = $SDCS_{coh}/SDCS_{incoh}$, for single electron capture for, 75 keV p + H_2. Here too, a clear structure is observed. A pronounced maximum can be seen at around 0 mrad followed by a minimum around 0.8 mrad and by another maximum at large angles. The structure seen here is quite similar to what was observed for R (see figure 2, paper I) for ionization of H_2 by 75 keV proton impact. One noticeable difference between the R for single capture and ionization is that, for single capture at 0 = 0 mrad, the ratio is 1, whereas in ionization the ratio is larger than 1. The reason for this is that, as mentioned earlier, in this experiment the angular distribution for the coherent and the incoherent cases were extracted simultaneously. The x- and y- axes, along which the coherent and incoherent scattering angle dependencies were measured, cross each other at 0 = 0 mrad. The number of counts in the pixel in the two dimensional position spectrum where this

crossing occurs thus represents the DDCS for θ = 0 mrad for both the coherent and incoherent case at the same time. Hence, in this particular experimental method, at θ = 0 mrad, the ratio R is forced to be 1, basically because the x- and y – directions are no longer defined at θ = 0 mrad. However in the ionization experiment, coherent and incoherent cross sections are measured separately, both in the x-direction, and therefore at θ = 0 mrad, R may be different from 1.

The similarity of R between single capture and ionization implies that this structure is also due to Young type interference. An interference pattern is present when the beam is coherent and it is not present when the beam is incoherent. Hence this is another demonstration of the effect of projectile coherence on the measured cross sections.
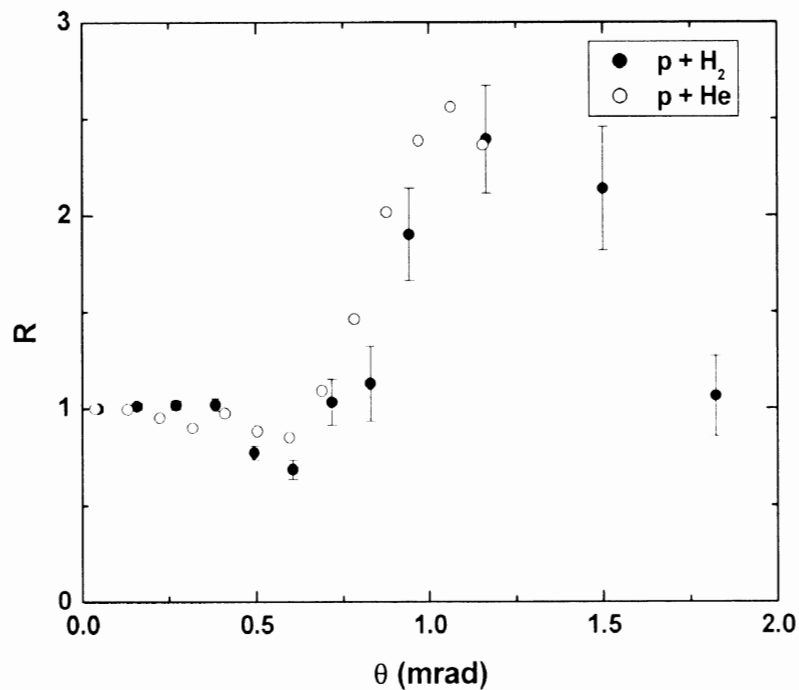

Figure 2.3 The ratio, R=SDCS$_{coh}$ / SDCS$_{inc}$ for single electron capture by 25 keV proton on H$_2$ (solid symbols) & He (open symbols)

Further, the experiment was repeated for the same conditions, but for an impact energy of 25 keV. The corresponding R is shown in figure 3.3 for a H_2 target as solid symbols and a He target as open symbols. These data are qualitatively different from the 75 keV p + H_2 data. But interestingly, the ratios for both H_2 and He exhibit structures which are very similar to each other. For small angles (up to about 0.4 mrd) the ratios remain flat, at R=1, and approach a minimum around 0.6 mrad followed by a pronounced maximum around 1 mrad. The structure indicates the presence of some type of interference. However the fact that these are quite different from the structures observed for 75 keV p+ H2 and that they occur for an atomic target imply that these are not due to Young type interference.

The presence of the structure for He demonstrates that the projectile coherence can have an observable effect on measured cross sections for atomic targets as well. It is not yet clear what type of interference causes this structure, but one possibility is the occurrence of path interference between two different impact parameters which lead to the same scattering angle depending on whether the N-N contributes significantly to the scattering or not. Such structures have been predicted in theory [31], but only have been experimentally observed for collisions with smaller projectile energies [32]. For large energies theory predicts the structure to become weaker. In addition they may have not been observed since at larger energies the projectile may have been incoherent. The present data are the first demonstration of such structures for an impact energy as large as discussed here.

3. CONCLUSIONS

The first part of this dissertation described an experiment performed to investigate the effect of projectile coherence on measured cross sections for ion impact. The double differential cross sections were measured for single ionization of molecular hydrogen by 75 keV proton impact for a coherent projectile beam and an incoherent projectile beam. Clear differences were observed between the two data sets, where in the coherent data ($DDCS_{coh}$) a Young type interference structure was present, while in the incoherent data ($DDCS_{inc}$) it was not present. Further, the data were compared with the DDCS for ionization of atomic hydrogen, a Molecular Three Body Distorted Wave calculation (M3DW) [33] for a H_2 target, and a calculation based on a modification of Second Born Approximation calculation with a Coulomb Waves (SBA-C) for an atomic hydrogen target [34]. The M3DW calculation, which treats the projectile fully coherently, reproduced the $DDCS_{coh}$ very well. However, the same model was not able to reproduce the $DDCS_{inc}$. On the other hand the $DDCS_{inc}$ were in good agreement with the experimental DDCS for atomic hydrogen and also were very well reproduced by the SBA-C calculation, except for very large angles. Moreover, the interference term, which is the ratio, $DDCS_{coh}$ / $DDCS_{inc}$, clearly showed a structure and this structure was very well reproduced by the theoretical ratio between the M3DW calculation and the SBA-C calculation, except for very large angles due to the discrepancy between the $DDCS_{inc}$ and the SBA-C calculation for large angles.

Further, an experiment was performed to measure the SDCS for single electron capture by 75 keV and 25 keV proton impact for both a coherent and an incoherent projectile beam, where in this experiment it was possible to perform the experiment for

both the coherent and incoherent cases simultaneously. The ratio between the coherent

and incoherent cross sections for single electron capture by 75 keV proton impact on

molecular hydrogen clearly showed an interference structure, and this structure was quite

similar to the structure observed in the corresponding ratio for ionization of H_2 by 75 keV

protons. This is a clear indication that this structure is due to Young type interference

which was present when the projectile was coherent, and it was not present when the

projectile beam was incoherent. Moreover, similar measurements were performed for

impact of 25 keV protons on H_2 and He targets. However, in this case, the structures in

the ratio between the $SCDS_{coh}$ and $SDCS_{inc}$ were quite different to what was observed for

single electron capture for 75 keV p + H_2, and more importantly there is a structure for

He, which does not have two centers. This means that in this case Young type

interference structure was not present in this data. On the other hand, the presence of a

structure indicates that there must be some other type of interference because it implies

that here too the projectile coherence does have an effect on the observed cross sections.

Moreover, the fact that a structure is observed for He demonstrates that this type of

interference is relevant to an atomic target. Although the exact origin of these structures it

is not yet clear, one possible candidate is a path interference between two different

impact parameters which lead to the same scattering angle, depending on whether the N-

N interaction is present or not (figure 4.1). These have been predicted by theory [31], but

have been observed experimentally only for small projectile energies [32]. The reason for

this might be that for larger energies the projectile is not coherent. These data present the

first experimental demonstration of such type of interference at a projectile energy as
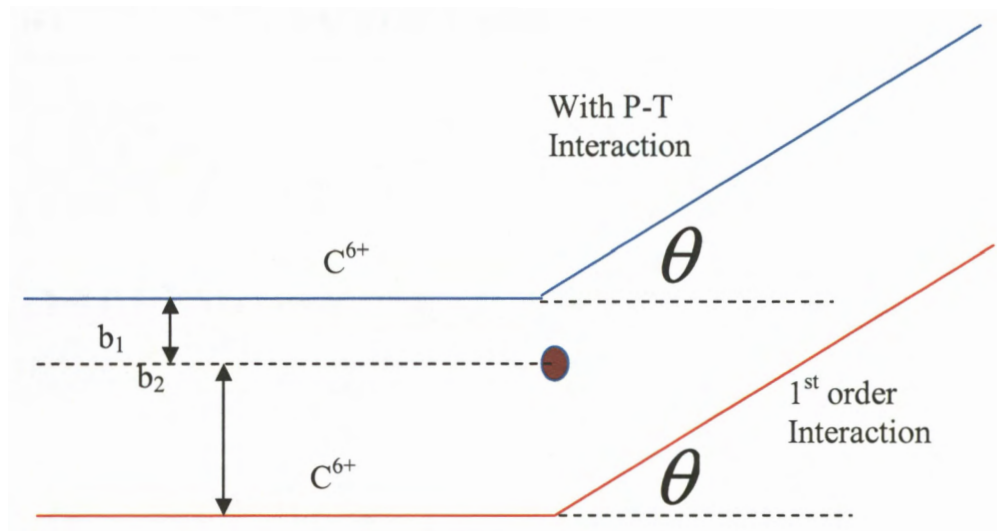
large as 25 keV.

Figure 3.1 Two impact parameters leading to the same scattering angle depending on the presence or absence on the N-N interaction.

The importance of the projectile coherence has been demonstrated in three different data sets. This implies that in theory the projectile must be represented by a localized wave packet, and the width of the wave packet should reflect the experimental beam conditions. For decades atomic collision theory assumed a fully coherent projectile beam. Although, this approximation has been successful in many cases, the results of this experiment clearly indicate that this is not sustainable in general, and further imply that a proper representation of the projectile might remove at least part of the discrepancies that have been observed between theory and experiment.

One such case is the discrepancy observed between experiment and state of the art fully quantum mechanical theories for ionization of He by impact of 100 MeV/a.m.u C^{6+}, which was described in the introduction of this dissertation. Previously it was thought that

even the relatively simple First Born Approximation would reproduce experimental data at such small perturbation. One possible explanation, for the discrepancies even by the most sophisticated calculations, similar to the explanation for the 25 keV p + He case, is that in fully quantum mechanical theory, where the projectile is treated coherently, two different impact parameters can lead to the same scattering angle depending on whether the nuclear-nuclaer interaction (N-N interaction) contributes significantly to the scattering or not (shown in figure 4.1). This can lead to an interference between these two terms. However the experimental width of the projectile wave packet was about 10^{-3} a.u., which is extremely small compared to the dimensions of the target atom. Therefore the interference between different terms in the theory is artificial, which would explain the discrepancy between the theory and the experiment.

Paper II describes an experiment where DDCS for dissociative ionization of H_2 by 75 keV proton impact was measured as a function of the projectile scattering angle for several energy losses. Several processes contribute to dissociative ionization. These are ground state dissociation (i.e. ionization accompanied by vibrational excitation of the H_2^+ molecule in the electronic ground state to a dissociative state), double excitation followed by auto ionization, ionization plus excitation and double excitation. Depending on the energy loss different processes were dominant. The cross sections observed in all of these processes were to a large extent similar to each other. However, for all four energy losses a frequency doubling of the angular dependence of the interference structure was observed compared to non-dissociative ionization. This is quite unexpected since the phase factor has only a weak dependence on the Q-value so that for a given scattering angle it should not differ significantly for different processes. Several reasons can

contribute to this doubling of the frequency. However from the data obtained from this experiment, it was not possible to come to a definite conclusion about the origin of this frequency doubling. One possibility is that the interference term, which was used to reproduce the non-dissociative ionization data, is not valid for dissociative ionization. In fact, this has been suggested previously in order to explain dissociative ionization data for electron impact [35]. Another possibility is that the peak seen around 0.7 mrad has a different origin which is not related to molecular interference structure. Similar peak structures have been observed exactly around the same angle in the cross section ratio between the two electron processes to that of the corresponding one electron process (e.g. double to single excitation). This might indeed be a very good explanation since most of the ratios observed in the interference term for dissociative ionization represent a ratio between the single electron process and a two electron process.

BIBLIOGRAPHY

[1] T.N. Rescigno, M. Baertschy, W.A. Isaacs, and C.W. McCurdy, Science **286**, 2474 (1999)

[2] M. Schulz, R. Moshammer, D. Fischer, H. Kollmus, D. H. Madison, S. Jones, and J. Ullrich, Nature **422** 48 (2003)

[3] M. Schulz and D. H. Madison, Int. J. Mod. Phys. A **21** 3649 (2006)

[4] H. Ehrhardt, K. Jung, G. Knoth, and P. Schlemmer, Z. Phys. **D1**, 3 (1986)

[5] A. Lahmam-Bennani, J. Phys. **B24**, 2401 (1991)

[6] R. Dörner, V. Mergel, R. Ali, U. Buck, C.L. Cocke, K. Froschauer, O. Jagutzki, S. Lencinas, W.E. Meyerhof, S. Nüttgens, R. E. Olson, H. Schmidt-Böcking, L. Spielberger, K. Tökesi, J. Ullrich, M. Unverzagt, and W. Wu, Phys. Rev. Lett. **72**, 3166 (1994)

[7] R.Moshammer, M. Unverzagt, W. Schmitt, J. Ullrich, H. Schmidt-Böcking, Nucl. Instrum. Meth. B **108**, 425 (1996)

[8] M. Schulz, R. Moshammer, A.N. Perumal, and J. Ullrich, J. Phys. B **35**, L161 (2002)

[9] N.V. Maydanyuk, A. Hasan, M. Foster, B. Tooke, E. Nanni, D.H. Madison, and M. Schulz, Phys. Rev. Lett. **94**, 243201 (2005)

[10] H. Kollmus, R. Moshammer, R.E. Olson, S. Hagmann, M. Schulz, and J. Ullrich, Phys. Rev. Lett. **88**, 103202 (2002)

[11] V. Mergel, R. Dörner, Kh. Khayyat, M. Achler, T. Weber, O. Jagutzki, H.J. Lüdde, C.L. Cocke, and H. Schmidt-Böcking, Phys. Rev. Lett. **86**, 2257 (2001)

[12] A. Hasan, B. Tooke, M. Zapukhlyak, T. Kirchner, M. Schulz, Phys. Rev. A **74**, 032703 (2006)

[13] M. Schulz, Comments on Atomic, Molecular, and Optical Physics, Phys. Scr. 80, 068101 (2009)

[14] M. Dürr, C. Dimopoulou, B. Najjari, A. Dorn, K. Bartschat, I. Bray, D.V. Fursa, Z. Chen, D.H. Madison, and J. Ullrich, Phys. Rev. A **77**, 032717 (2008)

[15] I. Bray, Phys. Rev. Lett. **89**, 273201 (2002)

[16] Y. Fang and K. Bartschat, J. Phys. B **34**, L19 (2001)

[17] J. Colgan, M.S. Pindzola, G. Childers, and M.A. Khakoo, Phys. Rev. A **73**, 042710 (2006)

[18] T.-G. Lee, S. Yu. Ovchinnikov, J. Sternberg, V. Chupryna, D.R. Schultz, and J.H. Macek, Phys. Rev. A **76**, 050701 (2007)

[19] M.S. Pindzola, F. Robicheaux, and J. Colgan, J. Phys. B **40**, 1695 (2007)

[20] M. McGovern, C.T. Whelan, and H.R.J. Walters, Phys. Rev. A **82**, 032702 (2010)

[21] D Madison, M Schulz, S Jones, M Foster, R Moshammer and J Ullrich J. Phys. B 35 3297 (2002)

[22] M. Schulz, M. Dürr, B. Najjari, R. Moshammer, J. Ullrich, Phys. Rev. A **76**, 032712 (2007)

[23] T. F. Tuan and E. Gerjuoy, Phys. Rev. **117**, 756 (1960)

[24] S. Cheng, C. L. Cocke, V. Frohne, E. Y. Kamber, J. H. McGuire, and Y. Wang, Phys. Rev. A **47**, 3923 (1993)

[25] N. Stolterfoht, B. Sulik, V. Hoffmann, B. Skogvall, J. Y. Chesnel, J. Ragnama, F. Frèmont, D. Hennecart, A. Cassimi, X. Husson, A. L. Landers, J. Tanis, M. E. Galassi, and R. D. Rivarola, Phys. Rev. Lett. **87** 23201 (2001).

[26] N. Stolterfoht et al., Phys. Rev. A **67**, 030702 (2003)

[27] D. Misra, U. Kadhane, Y. P. Singh, L. C. Tribedi, P. D. Fainstein, and P. Richard Phys. Rev. Lett. **92**, 153201 (2004)

[28] D. Misra, H.T. Schmidt, M. Gudmundsson, D. Fischer, N. Haag, H.A.B. Johansson, A. Källberg, B. Najjari, P. Reinhed, R. Schuch, M. Schöffler, A. Simonsson, A.B. Voitkiv, and H. Cederquist, Phys. Rev. Lett. **102**, 153201 (2009)

[29] L. Ph. H. Schmidt, S. Schössler, F. Afaneh, M. Schöffler, K. E. Stiebing, H. Schmidt-Böcking, and R. Dörner, Phys. Rev. Lett. **101**, 173202 (2008)

[30] J. S. Alexander, A.C. Laforge, A. Hasan, Z.S. Machavariani, M.F. Ciappina, R.D. Rivarola, D.H. Madison, and M. Schulz, Phys. Rev. **A78**, 060701(R) (2008)

[31] M. Zapukhlyak, T. Kirchner, A. Hasan, B. Tooke and M. Schulz, Phys. Rev. **A 77**, 012720 (2008)

[32] L. K. Johnson, R. S. Gao, R. G. Dixson, K. A. Smith, N. F. Lane, R. F. Stebbings, and M. Kimura, Phys. Rev. A 40, 3626☐1989

[33] U. Chowdhury, M. Schulz, and D. H. Madison, Phys. Rev. A **83**, 032712 (2011)

[34] M. Schulz, A.C. Laforge, K.N. Egodapitiya, J.S. Alexander, A. Hasan, M.F. Ciappina, A.C. Roy, R. Dey, A. Samolov, and A.L. Godunov, Phys. Rev. A **81**, 052705 (2010)

[35] A. Senftleben, T. Pflüger, X. Ren, O. Al-Hagan, B. Najjari, D.H. Madison, A. Dorn and J. Ullrich, J. Phys. B **43**, 081002 (2010)

VITA

Kisra Nayomal Egodapitiya was born and raised in Kandy, Sri Lanka. He attended St. Anthony's College in Kandy for his primary education. Then he entered the University of Peradeniya in Sri Lanka for his undergraduate studies where he majored in physics. After graduating from the University of Peradeniya, he worked as a teaching assistant for one year at the same institution. Then he was enrolled at the University of Missouri- Rolla (now Missouri University of Science & Technology) to pursue his PhD in physics. He joined the group of Dr. Michael Schulz to conduct research in the filed of experimental atomic collisions and earned his PhD in December 2011.

While at Missouri S&T, Kisra published four peer-reviewed journals papers. He also presented his research work at four international conferences. He was an invited speaker at the 2011 International Symposium on (e,2e), Double Photo-ionization & Related Topics & 16th International Symposium on Polarization & Correlation in Electronic & Atomic Collisions held in Dublin, Ireland. He won the runner-up at the 17th and 3rd place at the 18th Annual Laird D. Schearer Prize Competition held by the Missouri S&T physics department.